REVIEW

Detection of Kidney Disease Biomarkers based on Fluorescence Technology

Received 00th January 20xx,
Accepted 00th January 20xx

DOI: 10.1039/x0xx00000x

Bicheng Yao, Marie-Claire Giel and Yuning Hong *

Screening for kidney diseases is of vital importance due to their current prevalent worldwide. The diagnosis and monitoring of kidney diseases rely on kidney disease biomarkers (KDBs), which include traditional KDBs such as serum creatinine and proteinuria as well as novel biomarkers such as kidney injury molecule-1 (KIM-1), lipocalin 2 (NGAL), *N*-acetyl-β-D-glucosaminidase (NAG), cystatin C, etc. The latter has been highly recognised for early and accurate diagnosis of kidney disease in the past decades. Fluorescence techniques have recently drawn considerable attention in the area of biomedicine due to the merits of high sensitivity, rapidity and cost efficiency. The combination of fluorescence technologies and KDBs has been proven by many researches to be a promising strategy for the prediction of kidney disease. Thus, in this review, we summarize recent advances of fluorescene technologies applied in the detection of traditional and novel KDBs. Due to the space limit, we have focussed on four traditional KDBs and eight novel KDBs as representatives. The design of anescent molecules, establishment of detection assays, and sensing mechanism of fluorescent probes are discussed in detail. Finally, future challenges and opportunities in this field are also analyzed. Through this review, we hope to inspire the discovery of novel fluorescence techniques with excellent performance in the early diagnosis of kidney diseases.

1. Introduction

Kidney diseases, including acute kidney injury (AKI), chronic kidney disease (CKD), autosomal dominant polycystic kidney disease (ADPKD), nephrotic syndrome, etc., are disorders that affect the normal functions of the kidneys.[1] Some kidney diseases can be fully cured with no or little sequelae. However, most nephrotic patients, such as those with lupus nephritis or IgA nephropathy, will experience chronic and irreversible damage to the kidney.[2-4] Among various kinds of kidney diseases, CKD is the most common and refers to all conditions of reduced kidney function lasting for more than three months. At the last stage of CKD, which is usually known as End-Stage Renal Failure (ESRD), patients will have a short life expectancy unless they receive kidney dialysis or transplantation.[5] Over the last decade, kidney diseases have become an important public health concern worldwide. In 2016, a study estimated that the global CKD prevalence was between 12% and 15% of the world population.[6] Moreover, around 3 million people in the world are currently suffering from ESRD.[5] Thus, it is highly important to develop effective approaches for the prevention, diagnosis, and treatment of kidney diseases.

Currently, clinical test methods for the diagnosis of kidney disease usually involve urinalysis, blood tests, renal imaging, and biopsy.[7] The urinalysis is an informative and non-invasive diagnostic tool which has been widely utilized in both the ambulatory and hospital settings. Among the various parameter obtained from a urinary test, some may be applied in the detection of specific kidney diseases. For example, the presence of albumin in urine, also known as albuminuria, is a signal of kidney damage in patients with diabetes, hypertension, and glomerular diseases.[8] Besides urinalysis, blood tests are another important method to measure kidney function. Through the test of the serum concentration of an endogenous renal filtration marker (creatinine, cystatin C, etc.), the glomerular filtration rate (GFR), which is considered as the best overall indicator of kidney function, can be calculated using a special formula.[9] With the GFR value, clinicians can thereby determine patients' level of kidney function and stage of the kidney disease. Another commonly used renal test is imaging which includes ultrasound, computed tomography (CT) scan, etc.[10] These techniques are usually utilized for the diagnosis of kidney diseases like ADPKD, which causes many fluid-filled cysts to grow in the kidneys and change their shapes. Finally, kidney biopsy is applied when the kidney problem cannot be identified otherwise. Kidney diseases such as nephrotic syndrome, rapidly progressive glomerulonephritis, IgA nephropathy are usually evaluated via renal biopsy.

Even though remarkable progresses have been made in diagnostic techniques in the past century, early detection of kidney disease remains challenging. The difficultly in detection results from few or no symptoms present in patients with CKD at the early stage and many of the early signs of renal failure can be confused with other illnesses. As a result, most patients with kidney disease are confirmed at late stage with symptomatic kidney damage. In order to prevent or at least delay kidney disease from developing into severe kidney failure, early

Department of Chemistry and Physics, La Trobe Institute for Molecular Science, La Trobe University, Victoria 3086, Australia. E-mail: y.hong@latrobe.edu.au

diagnosis of kidney injury is highly important. For this purpose, kidney disease biomarkers (KDBs) are usually applied since they can provide better information about the status of ongoing renal injury and predict the likelihood of progression of kidney diseases. In the past decades, there has been increasing interest in exploring new biomarkers for kidney diseases.[11-17] As shown in **Scheme 1**, some typical KDBs are presented with corresponding injury sites along the nephron.[11] Among these KDBs, serum creatinine (sCr), blood urea nitrogen (BUN), proteinuria (including albumin, transferrin, β2-microglobulin, etc.) are clinically used to evaluate and monitor renal damage. Thus, they were classified as traditional KDBs. However, the sensitivity of these biomarkers is insufficient in many clinical scenarios. For example, the value of sCr remains within the normal range until more than 50% of the normal renal function is lost.[18-21] Additionally, the value of sCr can be influenced by multiple non-renal factors, such as age, gender, muscle mass, and diet. In order to overcome these limitations, novel biomarkers were developed including cystatin C, kidney injury molecule-1 (KIM-1), neutrophil gelatinase-associated lipocalin (NGAL), etc. These biomarkers have been demonstrated more sensitive and reliable than traditional KDBs, thus are believed to replace traditional KDBs gradually in the future.

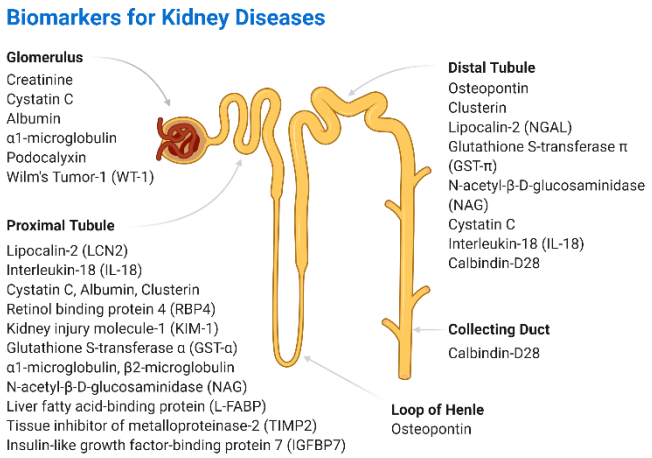

Scheme 1. Representative biomarkers of kidney disease with corresponding injury sites along the nephron.

Most of the KDBs, as shown in Table 1, are essentially proteins which are usually measured by mass spectrometry (MS), electrophoresis, or immunoassays. Although these techniques offer the advantage of high sensitivity and good accuracy, these methods usually require sophisticated instrumentation and the operation can be time-consuming and costly. Fluorescence techniques are expected to be a good alternative to the present KDB test techniques, due to their sensitivity, simplicity, rapidity, and cost efficiency.[22] The most commonly used fluorophores include fluorescent proteins, inorganic semiconductor quantum dots (QDs), organic dyes, and so forth.[23-26] Among these different types of fluorescent materials, small molecule organic fluorophores are the most commonly used, owing to their versatility for a wide range of functionality and applications. Classic organic fluorophores such as fluorescein, coumarin, BODIPY, rhodamine, etc. suffer from the aggregation-caused quenching (ACQ) effect.[27] The fluorescence intensity decreases dramatically when the fluorescent molecules are used at high concentration or in the solid state. This ACQ effect greatly compromises the performance and application of organic dye as biosensors in many scenarios. The novel concept of aggregation-induced emission (AIE), which is diametrically opposite to the ACQ effect, provides the solution to tackle the ACQ problem.[28] This concept depicts a class of propeller-shaped molecules which are non-emissive when molecularly dissolved in solutions but become highly fluorescent upon aggregate formation. After nearly two decades of developments in AIE research, AIE fluorogens (AIEgens) have been proven to have many advantages such as good photostability, broad working concentration range, large Stokes shifts, low background noise, etc. Therefore, AIE has become a hot research topic and been successfully applied in various fields such as optoelectronic devices, biosensing, imaging and tracking, phototheranostics, stimuli responsive materials, etc.[29-38]

Thanks to the continuous endeavours from researchers in areas of both KDB and fluorescence technology, many examples of fluorescence techniques applied in the detection of KDBs have been reported. In this review, recent research progress in the detection of KDBs using fluorescence techniques will be summarized. Due to the large amount of KDBs, only a selection of typical biomarkers will be introduced and discussed here. Particular emphasis will be placed on the design of fluorescent probe molecules and establishment of detection assays. Since AIEgens have many merits over traditional fluorophores, we will also emphasize AIE related work to motivate the development of fluorescent KDB probes with superb performance. Finally, we will draw a perspective on future development of fluorescence technology in the detection of KDBs.

Table 1. Kidney Disease Biomarkers along with their corresponding injury sites, kidney diseases and detection methods.

Kidney Disease Biomarker	Injury Site [a]	Related Kidney Disease [b]	Detection Method [c]	Ref.
Albumin	A, B	CKD and AKI	Immunoturbidimetry	39
Angiotensinogen (AGT)	-	AKI	ELISA	40
Apolipoprotein A-IV (ApoA-IV)	-	CKD	ELISA	41
Asymmetric dimethylarginine (ADMA)	-	CKD	HPLC	41
Blood urea nitrogen (BUN)	-	CKD and AKI	Colorimetry	41
Calprotectin	E	AKI	ELISA	42
CD14 mononuclear cells	-	PKD	ELISA	43
Clusterin	B, C	AKI, nephrotoxicity, PKD, fibrosis	ELISA	44
Connective tissue growth factor (CTGF)	B	DN	ELISA	41
Creatinine	A	CKD and AKI	Colorimetry	45
Cystatin C	A, B, C	CKD and AKI	ELISA, nephelometer	45
Cysteine-rich protein (Cyr61)	B	ischemic AKI	Western blot	44
Epidermal growth factor (EGF)	C	DN, IgAN, PKD	ELISA	45
Fetuin-A	B	ADPKD and AKI	Immunoblotting	44, 46
Fibroblast growth factor 23 (FGF-23)	-	CKD	2nd generation C-terminal assay	47, 48
Glutathione S-transferase α (GST-α)	B	nephrotoxicity and AKI	ELISA	47
Glutathione S-transferase π (GST-π)	C	nephrotoxicity and AKI	ELISA	47
Insulin-like growth factor-binding protein 7 (IGFBP7)	B	AKI	fluorescence immunoassay (NephroCheck™ Test)	47, 49
Interleukin-18 (IL-18)	B, C	AKI	Luminex®-based assay	47
Kidney injury molecule-1 (KIM-1)	B	CKD, AKI, and nephrotoxicity	Luminex®-based assay	45
Lactate dehydrogenase (LDH)	-	nephrotoxicity	Colorimetry	12
Lipocalin-2 (LCN2) or Neutrophil gelatinase–associated lipocalin (NGAL)	B, C	AKI, CKD, and LN	Luminex®-based assay	45
Liver fatty acid-binding protein (L-FABP)	B	CKD, AKI, DN, IgAN, and CIN	ELISA	
microRNA	-	CKD and AKI	Quantitative RT-PCR	50, 51
Monocyte chemoattractant protein-1 (MCP-1)	-	DN and LN	ELISA	45, 52
N-acetyl-β-D-glucosaminidase (NAG)	B, C	CKD, AKI, DN, and nephrotoxicity	Colorimetry	44
Netrin-1	B	AKI	ELISA	53
Osteopontin (OPN)	B, C, D	AKI, inflammation, and fibrosis	ELISA	44
Podocalyxin	A	MN, IgAN, and FSGS	flow cytometry	54
Procollagen type III N-terminal propeptide (PIIINP)	-	renal fibrosis	radioimmunoassay	45, 55
Retinol binding protein 4 (RBP4)	B	AKI, TIN, FS, and tubule dysfunction	ELISA, nephelometer	41
Tumor necrosis factor receptors (TNFR)	-	DN	ELISA	45
Symmetrical dimethylarginine (SDMA)	A	CKD	LC-MS	56
The sodium-hydrogen exchanger isoform 3 (NHE3)	B	AKI and prerenal azotaemia	Immunoblotting	44
Tissue inhibitor of metalloproteinase 2 (TIMP2)	B	AKI	fluorescence immunoassay (NephroCheck™ Test)	49, 57
Uromodulin or Tamm-Horsfall protein	B, C, D	CKD, tubular mass and function	ELISA	45
Wilm's Tumor-1 (WT-1)	A	DN	Western blot	58
α1-Microglobulin	B	tubular injury or dysfunction	ELISA, nephelometer	45
β2-Microglobulin	A, B	CKD, AKI, and nephrotoxicity	ELISA, nephelometer	41, 44
β-Trace protein (BTP)	A	CKD	Immunoturbidimetry	59
γ-Glutamyl transpeptidase (GGT)	B	AKI and nephrotoxicity	Colorimetry	44

Abbreviations: [a] Injury Site of Nephron: A, glomerulus; B, proximal tubules; C, distal tubules; D, loop of henle; E, collecting duct. [b] Related Kidney Disease: CKD, chronic kidney disease; AKI, acute kidney injury; PKD, polycystic kidney disease; DN, diabetic nephropathy; IgAN, IgA nephropathy; ADPKD, autosomal dominant polycystic kidney disease; LN, lupus nephritis; CIN, contrast-induced nephropathy; MN, membranous nephropathy; FSGS, focal segmental glomerulosclerosis; TIN, tubulointerstitial nephritis; FS, Fanconi syndrome. [c] Detection Method: ELISA, enzyme-linked immunosorbent assay; HPLC, high-performance liquid chromatography; RT-PCR, reverse transcription-polymerase chain reaction; LC-MS, liquid chromatography–mass spectrometry.

2. Application of Fluorescence Technologies in the Detection of Traditional KDBs

Traditional KDBs include sCr, albumin, transferrin, α1-microglobulin, β2-microglobulin, and so on. Based on our literature survey, fluorescence techniques have been applied in detecting some of these biomarkers, aiming to improve their detection sensitivity and clinical application capability. In this section, we will focus on the works of albumin, creatinine, transferrin and transferrin receptor detection by fluorescence methods.

2.1 Human Serum Albumin (HSA)

Human Serum Albumin (HSA) is the most abundant plasma protein in human's blood circulatory system. It is composed of a polypeptide chain with three α-helical domains (I-III).[60] Each of these domains can be further divided into two subdomains A and B. Due to the ligand-binding sites located in the hydrophobic cavities of subdomains IIA and IIIA, HSA exhibits an outstanding binding capacity for loading and transporting a wide range of biomolecules.[60-63] Moreover, the presence of excess HSA in urine (more than 30 mg/L) has been recognized as an indicator of kidney injury resulting from diabetes mellitus and hypertension. Therefore, detection of HSA in urine samples is of obvious value for the diagnosis of kidney diseases.

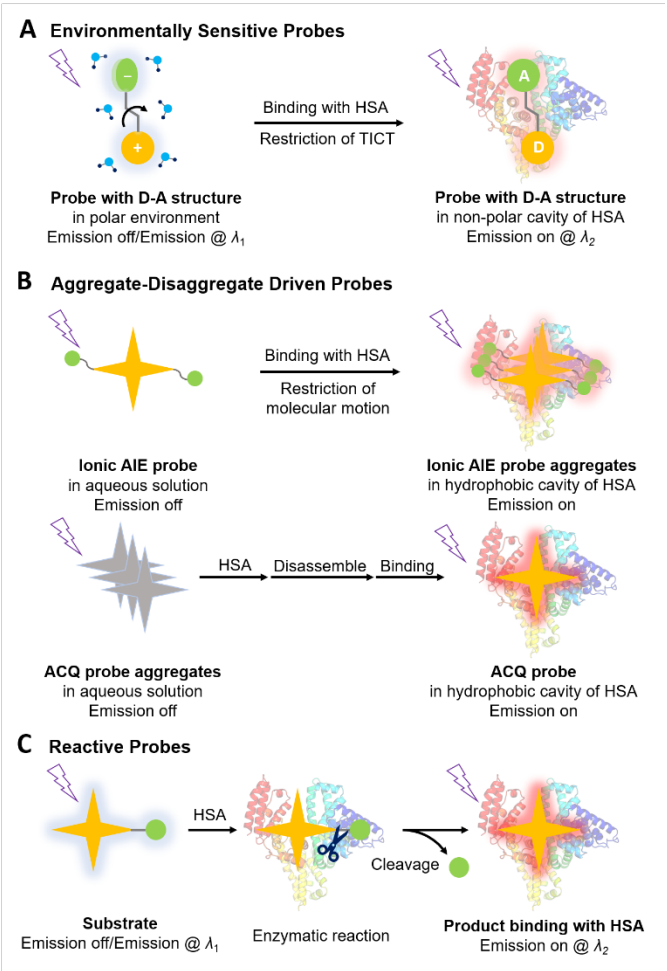

Scheme 2. Summary on working mechanisms of turn-on fluorescent probes for HSA detection. (A) Environment sensitive probes: Fluorescence of these probes with electron Donating–Accepting (D-A) structures can be modulated after entering the non-polar cavities of HSA from the polar aqueous environment. (B) Aggregate-disaggregate driven probes: These probes can be aggregated or disassembled through interactions with HSA and exhibit changes in fluorescence property. (C) Reactive probes: These probes containing aromatic amides or esters can undergo hydrolysis in the presence of HSA due to its pseudo-esterase activity.

Usually, albuminuria can be assessed using a semiquantitative urine dipstick which is easy to operate and low-cost. However, this method is not sensitive enough when albuminuria is moderately increased in the range of 30 to 300 mg/L (microalbuminuria). In this case, quantitative test techniques such as capillary electrophoresis and immunoassays are commonly used. These methods are more accurate, but expensive and time-consuming. To achieve fast response, high sensitivity and easy operation, fluorescence technique has been employed in the detection of HSA. In the past decades, there have been numerous organic fluorescent probes developed for HSA detection.[64, 65] These probes are mainly based on the following three working mechanisms (**Scheme 2**): (1) *environmentally sensitive probes* that can modulate their fluorescence emission intensity or wavelength when entering the nonpolar cavities of HSA from the polar aqueous environment, (2) *aggregate-disaggregate driven probes* which can be assembled or disassembled through interactions with HSA and exhibit changes in fluorescence readout, and change the fluorescence property, and (3) *reactive probes* which can undergo hydrolysis in the presence of HSA due to its pseudo-esterase activity.[66] As space is limited, only representative examples of HSA fluorescent probes in past ten years will be discussed in this review (**Scheme 3**).

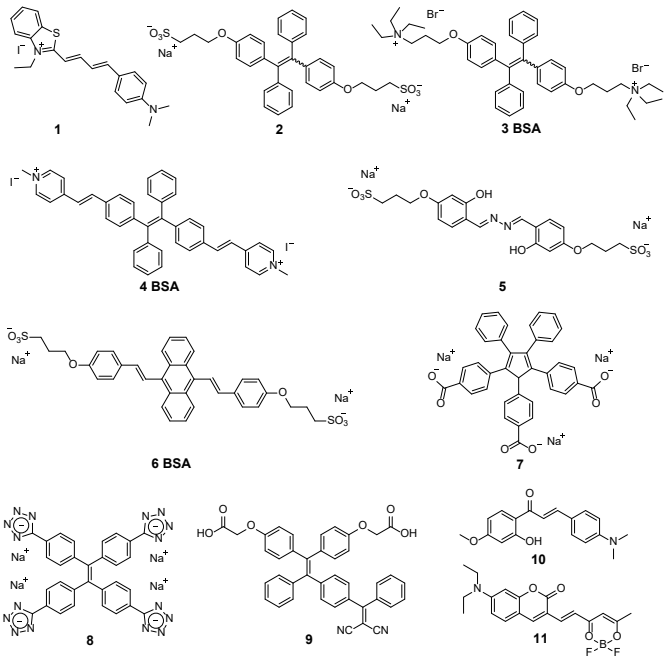

Scheme 3. Chemical structures of representative fluorescent probes **1**-**11** for the detection of HSA/BSA.

In 2016, Peng and co-workers reported a hemi-cyanine based probe **1** (**Scheme 3**) which is an environmentally sensitive probe showing obvious fluorescent response to HSA.[67] Probe **1** has a strong electron push-pull structure with the positive charge on the nitrogen atom as the acceptor and alkylamino group as donor that can undergo intramolecular charge transfer (ICT) process. As a result, the fluorescence of probe **1** is sensitive to the polarity changes of the surrounding environment. The fluorescence analysis revealed that the aqueous solution of probe **1** was almost non-emissive, possibly due to the effective twisted intramolecular charge transfer (TICT) effect. However, upon the addition of HSA, the fluorescence of probe **1** at 680 nm was gradually enhanced when excited at 580 nm. This can be ascribed to the transfer of probe **1** from polar aqueous solution to non-polar cavities of HSA, restricting the occurrence of TICT process. Furthermore, the detection limit of probe **1** was calculated as 1.73 mg/L in PBS buffer, and good linear relationship between the fluorescence intensity and HSA concentration can be obtained in both PBS buffer and real human urine.

The hydrophobic nature of the HSA interdomain cavity also allows AIEgens to bind or/and accumulate, which switches on their fluorescence as a result of restriction of intramolecular motions (RIM). AIE-active HSA probes can therefore be regarded as aggregate-disaggregate driven probes. Since first applied in the detection of albumin in 2006, various AIEgens have been developed for sensing albumins, including Bovine Serum Albumin (BSA) which acts as a substitute for HSA.[68-73] Some representative AIEgens (probe **2**-**7**) for albumin detection are shown in **Scheme 3**.[74-79] In general, these AIEgens are composed of an AIE core and periphery-charged groups such as anionic sulfonate and carboxylate groups or cationic trialkyl-ammonium and pyridinium groups. Although these probes showed good performance in laboratory environment, their sensitivity is still lower than what is required to use in a clinical setting, which can be attributed to the relatively low binding affinities to albumin.

Recently, Tu et al. reported a novel AIEgens **8** (**Scheme 3**) for HSA detection.[66] Based on the abovementioned design principle, tetraphenylethylene (TPE), a typical AIE chromophore, was selected as the AIE core. Meanwhile, tetrazolate was used as the charged moiety which not only improved the probes' water solubility to lower the background noise but also promoted their interaction with HSA. Unlike previously used ionic groups, the tetrazolate exhibited enhanced lipophilicity which led to a stronger binding affinity toward HSA. As a result, probe **8** showed superior performance in comparison to previously reported fluorogenic albumin probes. By plotting the peak fluorescence intensity versus the HSA concentrations, probes **8** was highly sensitive toward HSA with a broad linear dynamic range (LDR) and a low limit of detection (LOD). Additionally, when working in PBS buffer with a concentration of 5 μM, probe **10** exhibited the best performance with a LOD of 0.21 nM and LDR of 0-230 mg/L. Furthermore, by adjusting the probe concentration to 125 μM, the LDR of probe **8** can be tuned up to 3000 mg/L which can cover the range of HSA in most clinical urine and blood samples. Finally, in order to examine the feasibility of this fluorogenic assay, urine samples from hospital were analysed using probe **8**. The fluorescence analysis results indicated that probe **8** is capable of detecting urinary albumin quantitatively especially within the microalbuminuria range.

In 2016, Yu et al. constructed nanostructures using AIEgen **9** for detecting HSA.[80] As shown in **Scheme 3**, probe **9** contains three main moieties comprising the bulky and aromatic TPE unit which prefers the binding toward hydrophobic cavities of HSA, two carboxyl groups which help recognize cationic amino acids from HSA, and an electron accepting cyano group which was designed to adjust the emission to long-wavelength region. When dispersed in PBS buffer, probe **9** can spontaneously assembled into nanospheres with an average diameter of 34 nm. These nanospheres are non-fluorescent probably due to the loose molecular packing and TICT effect in the polar solvent. After the addition of HSA, the nanospheres disassembled in 5 min, and the free probe molecules can enter the binding sites of HSA. Afterwards, red emission signal would be observed under UV light due to the RIM mechanism of AIEgens.[30] Therefore, this probe can be used as a nano sensor for the detection of HSA.

Most recently, Luo et al. reported a ratiometric probe **10** (**Scheme 3**) based on the strategy of HSA induced disassembly of probe aggregates.[81] Different from abovementioned probes which displayed only fluorescence intensity changes upon incubation with HSA, probe **10** showed an obvious fluorescence emission colour change from red to green when encountering HSA. The red fluorescence of probe **10** can be ascribed to the excited-state intramolecular proton transfer (ESIPT) process in solid/aggregated state. Upon titration of HSA, the aggregates of probe **10** disassemble and the individual molecules interact with HSA which results in the shift of red to green emission. It was observed that probe **10** displayed a 24-fold change from 0.198 to 4.78 in the emission intensity ratio (I_{520}/I_{620}) against the HSA concentration ranging from 0 to 15 μM. Moreover, the LOD was calculated to be 16.4 nM (1.08 mg/L) with an LDR (R^2 = 0.995) between 0 and 9 μM. Dynamic light scattering analysis further proved the sensing mechanism of probe **10** to be the HSA induced disassembly of aggregates. Probe **10** was further integrated with the microfluidic paper-based analytical device (μPAD) to form a point-of-care (POC) device for HSA detection in both MilliQ water and whole blood samples. A linear relationship (R^2 = 0.95) was retained between HSA concentration and the emission intensity ratio when the μPAD system was applied in whole blood. This work provides a cost-effective detection platform for POC HSA monitoring.

Finally, a reactive probe that underwent hydrolysis in the presence of HSA was reported by Sun et al. in 2017.[82] As shown in **Scheme 3**, probe **11** was constructed by conjugating a dioxaborine with a polarity-sensitive coumarin fluorophore. Due to the electrical push-pull structure, probe **11** absorbs and emits in the long wavelength region. Owing to the pseudo-esterase activity of HSA, the dioxaborine group can be hydrolysed in the cavity of HSA, resulting in remarkable fluorescence enhancement along with a notable blueshift. The data presented in this work showed that probe **11** absorbs at

515 nm and is non-emissive in PBS buffer. Once upon the addition of 1.0 mg/mL HSA solution, the absorption peak at 515 nm decreased gradually accompanied by the appearance and development of a new band peaked at 475 nm. Furthermore, a broad emission band with two peaks at 540 and 585 nm emerged within 1 min, and the one at 540 nm kept increasing dramatically within 15 min, showing a 1000-fold fluorescence enhancement. Thus, probe **11** could be applied for the fast and sensitive detection of HSA. The detection mechanism was further manifested via UPLC-MS and comparison of probe **11** with its hydrolysis product.

In summary, fluorescent HSA probes have developed rapidly in the past decade, showing improved sensitivity and specificity. Some of these probes were proved to detect HSA in real serum and urine samples. However, due to the nonspecific binding force (hydrogen bonding, hydrophobic interaction, and π- π interaction) between these probes and HSA, fluorescent probes can be interfered by other substances in the biofluids, such as creatinine. Therefore, further improvement in the specificity of fluorescent probes towards HSA in real clinical samples is still required.

2.2 Creatinine

As mentioned above, creatinine, a breakdown product of creatine and phosphocreatine from muscle metabolism, is another important component in human blood and urine. It is transported through the bloodstream to the kidney, filtered by glomerular filtration, and finally excreted in the urine. The normal level of creatinine for an adult is 45-110 μmol/L in serum and 5.3-17.7 mmol/24h in urine.[83] Once the renal filtration function is deficient, the blood creatinine concentration will increase. Therefore, the creatinine concentration in blood may be used to calculate the GFR which is clinically important to evaluate kidney function.[83] Furthermore, since the daily excretion amount of creatinine is constant for a healthy person, the concentration of a spot urine can be corrected via measuring its creatinine concentration. Thus, the influence of the spot urine concentration on urine albumin test can be eliminated by applying the Urine Albumin-to-Creatinine Ratio (UACR) test. Therefore, creatinine represents an important KDB regardless if detected in blood or urine.

Currently, the colorimetric Jaffe assay is the most commonly technique in clinical laboratories to determine creatinine levels in blood and urine.[84] In a Jaffe reaction, the reactive methylene group of creatinine reacts with sodium picrate in alkaline medium, forming a reddish-orange complex with a maximum absorbance at around 520 nm. This colour change was proportional to the concentration of creatinine, thus can be used for creatinine quantification.[85-87] The LOD of Jaffe assay was determined as 0.1 and 0.25 mg/dL in serum and urine, respectively.[88] Even though it is simple, adaptable in automated analysis, and cost-effective, Jaffe assay's non-specificity continues to be a limiting factor of the technique. In the presence of interferents, such as glucose, acetoacetate, proteins, ascorbic acid, hemolysis, nonspecific chromogenic reaction may occur, causing falsely elevated creatinine results.[89] Therefore, the development of new and efficient methods for creatinine analysis is highly demanded.

In recent years, there are several fluorescent materials developed for the sensing of creatinine. In 2017, Tang and co-workers reported an AIE-active creatinine probe **12**.[90] As shown in **Scheme 4**, this probe was designed using the iminodiacetic acid to modify the TPE core. Thanks to this special structure, probe **12** was able to easily coordinate with creatinine via hydrogen bond interactions between the amine groups of creatinine and the carboxyl acid groups of **12**. As a result of binding with a large group, the emission of probe **12** was enhanced due to the RIM mechanism. Therefore, this probe can be utilized for the detection of creatinine. In addition, the authors also applied probe **2** (**Scheme 3**) as the HSA probe and studied the mutual interference of creatinine and HSA during detection and quantitation in artificial urine.

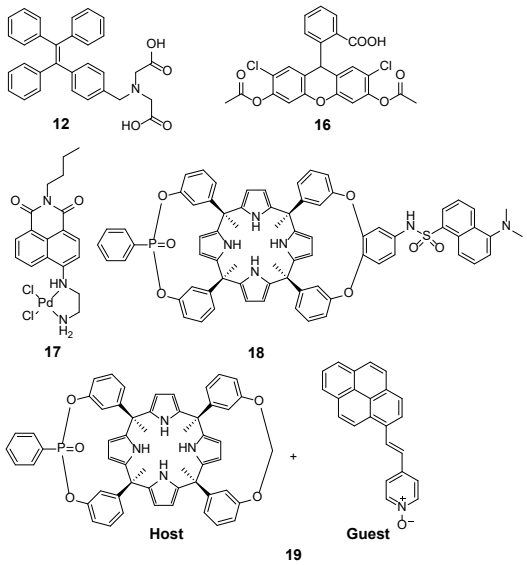

Scheme 4. Chemical structures of creatinine probes **12**, and **16**-**19**.

Recently, fluorescent noble metal nanoclusters have drawn considerable interest from biosensing area due to their strong luminescence, ultrafine size, good biocompatibility, etc.[91] In 2017, Joseph and Mathew reported gluten (a cysteine-rich protein) stabilized fluorescent gold nanoclusters (AuNCs) which can be applied in the detection of creatinine.[92] The schematic of the synthesis and sensing mechanism of AuNCs (probe **13**) is shown in **Scheme 5A**. By mixing gluten and $AuCl_4$ under basic pH and stirring at 55 °C for 3h, probe **13** with an average diameter around 1.5 nm was formed exhibiting an emission peak centred at 680 nm when excited under 380 nm. The luminous mechanism of these nanoclusters was discussed by Tang and co-workers, suggesting that the fluorescence comes from a narrow band gap generated from inter-/intramolecular through space conjugation of protein ligands.[93] In order to establish a fluorescence turn-on sensing process, picric acid (PA) was first added to quench the red fluorescence of probe **13**. Afterwards, creatinine was introduced to form complexes with PA and restore the fluorescence of probe **13**. Through the fluorescence titration, the authors obtained a very good linear relationship between the fluorescence intensity of **13**-PA complex and the concentration of creatinine in the range of 20 to 520 μM.

Besides, the LOD of probe **13** was estimated to be 2 nM which is much lower than the normal level of creatinine in human blood. Finally, probe **13** was applied in blood samples spiked with various concentrations of creatinine and satisfying results were obtained, exemplifying its great potential for practical application. A similar study was reported by Rajamanikandan and Ilanchelian in 2018.[94] The researchers developed BSA modified copper nanoclusters (**14**) which emits red fluorescence for the optical recognition of creatinine. According to the authors, the fluorescence of probe **14** was considerably decreased by the addition of creatinine due to the formation of non-emissive coordination. Therefore, this probe can be utilized for the detection of creatinine. Recently, Khataee's group reported copper nanoclusters **15** which was capped with glutathione (GSH).[95] As shown in **Scheme 5C**, probe **15** will aggregate and emit red light in the presence of Al^{3+} ions, showing the typical AIE characteristic. Afterwards, on the addition of creatinine, the strong coordination interaction between creatinine and Al^{3+} ions led to the disassembly of aggregates, thus resulted in the fluorescence quenching. The quenched emission intensity exhibited a linear dependence on the concentrations of creatinine in the range of 2.5 to 34 µg/L with a LOD of 0.63 µg/L. Finally, this probe was applied in spiked human serum samples and gave satisfying results.

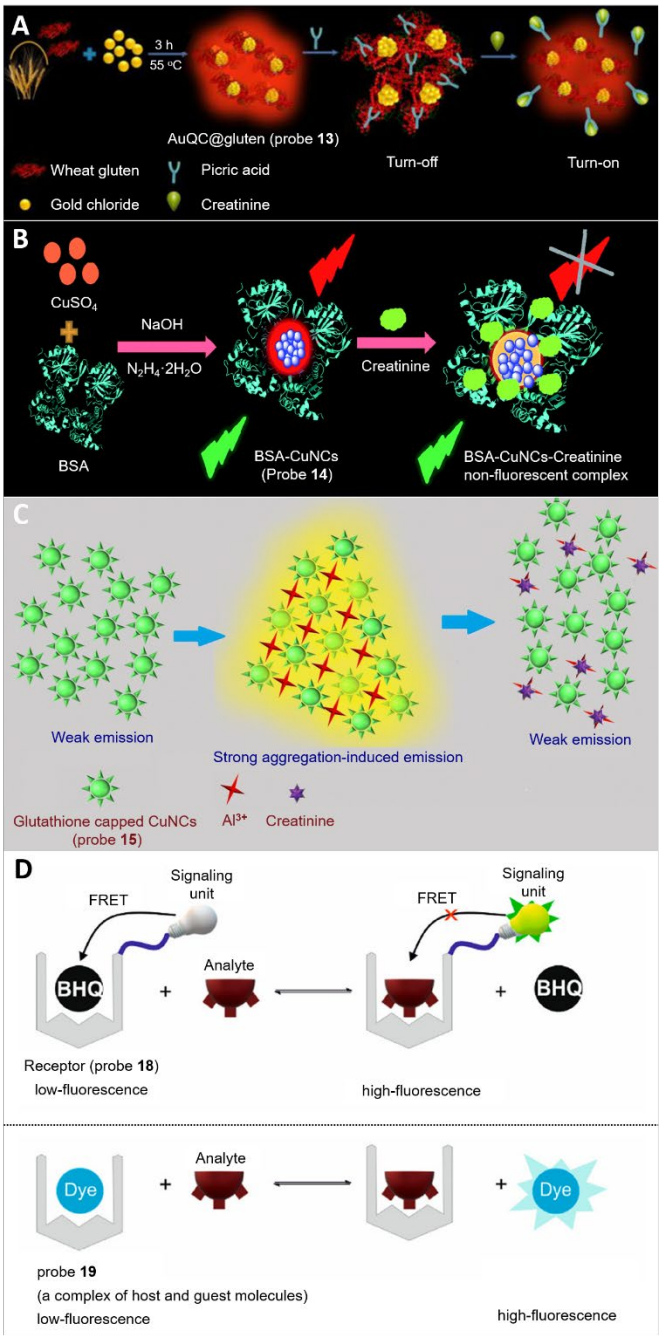

Scheme 5. Schematics of the sensing mechanism of A) probe **13**, B) probe **14**, C) probe **15** and D) probe **18** and **19**. A) Adapted with permission from ref. 92. Copyright 2017 American Chemical Society. B) Adapted with permission from ref. 94. Copyright 2018 The Royal Society of Chemistry. C) Adapted with permission from ref. 95. Copyright 2018 Springer-Verlag GmbH Austria, part of Springer Nature. D) Adapted with permission from ref. 96. Copyright 2020 American Chemical Society.

Besides the AIEgens and nanoclusters, traditional organic fluorophores like fluorescein, dansyl, naphthalene, and pyrene can be applied as a fluorescent reporter for creatinine sensing. In 2015, Nanda et al. reported the measurement of creatinine in human plasma using a functional porous polymer together with 2',7'-dichlorofluorescein diacetate (probe **16**, **Scheme 4**).[97]

This porous polymer was synthesized from two ionic liquids, poly-lactic-co-glycolic acid (PLGA) and 1-butyl-3-methylimidazolium (BMIM) chloride. After mixing the porous polymer, probe **16** and creatinine together, the ester-containing pore of porous polymer and OH^- produced from the hydrolysis of creatinine were able to convert probe **16** to ionized 2',7'-dichlorofluorescein. This product can emit green fluorescence in aqueous solution, which can therefore indicate the concentration of creatinine. Another work was presented by Chattopadhyay, Dhara and co-workers using a Pd^{2+}-naphthalimide based fluorescence light-up probe.[98] As shown in **Scheme 4**, probe **17** consists of a naphthalimide moiety which acts as the fluorescent ligand, and an ethylenediamine moiety complexing with Pd^{2+}. This probe exhibits very weak fluorescence due to the combination of heavy atom quenching effect, photoinduced electron transfer (PET) process, and the weakened ICT process caused by Pd^{2+}. However, after being treated with creatinine, Pd^{2+} coordinates with creatinine due to the greater affinity of creatinine towards the Pd^{2+} ion and free naphthalimide will be released to turn-on the fluorescence. The result of fluorescence titration further demonstrated that probe **17** could be employed in detecting creatinine with a wide range of linearity and a LOD of 0.30 μM. Furthermore, this assay has excellent selectivity over a variety of interfering metal ions, anions, and biologically species. Lastly, Sierra et al. reported an example of optical supramolecular sensing of creatinine.[96] Two strategies (**Scheme 5D**) were proposed based on the competitive Indicator Displacement Assay using Calix[4]pyrrole as the host molecule and pyridyl-*N*-oxide compounds as the guest molecules. In the first scenario, the highly emissive dansyl-modified calix[4]pyrrole (probe **18**) will form a low fluorescent supramolecule when complexing with the *para*-substituted pyridyl-*N*-oxide black-hole quencher (BHQ), which can quench the fluorescence of probe **18** through the Förster Resonance Energy Transfer (FRET) effect. Then the competitive displacement of the BHQ by creatinine can turn on the fluorescence of the host molecule. On the other hand, the unmodified calix[4]pyrrole phosphonate could be combined with the pyrene substituted pyridyl-*N*-oxide and form another low fluorescent complex (probe **19**). Then the fluorescence of guest molecule would be restored when it was replaced by the later added creatinine. Both two strategies were proved to have the ability to measure creatinine levels in clinically important ranges. However, there are still several drawbacks of this assay including poor sensing selectivity and low compatibility with aqueous media.

To summarize, much effort in developing novel fluorescent probes for sensing creatinine was motivated by the nonspecificity of Jaffe assay. The LOD of current fluorescent methods can be as low as 2 nM which is better than Jaffe assay. However, more clinical validations are necessary to further evaluate their performance in complex real clinical samples.

2.3 Transferrin and Soluble Transferrin Receptor

Transferrin (Tf) is a blood plasma glycoprotein with 679 amino residues and a molecular weight of ~80 kDa. It plays an important role in transporting ferric ions to various cells and tissues.[99] Due to its high molecular weight, Tf rarely passes through the glomerular membrane. Therefore, very few Tfs exist in the urine of a healthy person. For patients with diabetes, the abnormally high amount of blood glucose may cause damages to renal capillaries, as well as the selective barrier of glomerular filtration membrane. As a result, there will be an obvious increase in the Tf concentration of urine from diabetics.[16] Thus, urine Tf may be regarded as an early biomarker of glomerular injury.

At present, the most popular method for protein detection is mass spectrometry. Although this method enjoys the merits of high sensitivity and detection efficiency, the cost is also very high. Besides, protein MS usually needs sample pretreatment which may cause proteins to be hydrolyzed or denatured.[100] Recently, the molecular imprinted technique (MIT) has drawn great attention from the area of protein detection.[101] This technique usually applies a template molecule, functional monomer and crosslinking agent to prepare the molecular imprinted materials (MIM) which can form many cavities after removing the template molecules. These cavities have great selectivity towards the template molecules, thus can be used as a probe for certain kinds of analytes. In 2018, Zhang and co-workers reported a magnetic fluorescent molecular imprinted nanoparticle for the detection of Tf.[102] The synthesis of Tf probe **20** is shown in **Scheme 6A**. Firstly, the Fe_3O_4 nanoparticles were modified using 3-carboxybenzeneboronic acid in order to introduce the boronic acid moiety which can then bind with Tf. Then Tf was used as template molecule and ethylsilicate (TEOS) served as both functional monomer and crosslinker. After the completion of crosslinking reaction of TEOS, Tf molecules will be confined inside. Followed by removal of Tf and electrostatic adsorption of a semi-cyanine fluorogen CyA, probe **20** was finally obtained. This probe showed a strong near infrared (NIR) fluorescence emission at 730 nm while excited at 690 nm. After adding Tf, an obvious fluorescence quenching will occur due to the PET effect between electron-rich Tf and N^+ moiety of CyA. Therefore, the concentration of Tf can be determined by measuring the degree of decrease in the fluorescent signal. After optimizing experimental conditions, probe **20** exhibited excellent performance in detecting Tf, giving a lower relative standard deviation (7.7%), a good analytical range (0.025–0.175 mg/mL, R^2 = 0.998), and a low LOD (7.5 μg/mL). Furthermore, this method was also proved to have good selectivity towards Tf and can be applied to real sample analysis. Nevertheless, the non-linear curve obtained from the fluorescence quenching process remains a limitation of this method.

Transferrin receptor (TfR) is a membrane protein for Tf. The extracellular portion of TfR can be cleaved and released into serum producing the soluble Transferrin receptor (sTfR). In 2013, Delanghe et al. reported that urinary sTfR level might allow distinguishing IgA nephropathy and Henoch–Schönlein Purpura Nephritis (HSPN) from other causes of proteinuria. Hence, sTfR could be a potential biomarker to monitor IgA nephropathy and HSPN.[103] Recently, Tang, Liu and co-workers reported an example of AIEgen for the specific light-up sensing of sTfR.[104] As shown in **Scheme 6B**, the probe **21** mainly consists of three elements, a TPE core as the fluorescence reporter

emitting green light, a peptide T7 (His-Ala-Ile-Tyr-Pro-Arg-His, HAIYPRH) moiety allowing specific binding with sTfR, and alkyne and azide groups facilitating the covalent conjugation between the TPE and peptide. Thanks to the peptide moiety, probe **21** displays good water solubility which makes it almost non-emissive in aqueous solution. In contrast, the fluorescence of probe **21** was enhanced dramatically upon interaction with sTfR. Therefore, this probe can be used for the light-up detection of sTfR. The sensing mechanism of this probe can be attributed to the RIM process of TPE upon binding to sTfR. After measuring fluorescence intensity change of probe **21** in the presence of sTfR, the LDR and LOD were calculated as 0-80 μg/mL and 0.27 μg/mL, respectively. In addition, the excellent selectivity of probe **21** was also examined by incubating it with other proteins including pepsin, lysozyme, HSA, and Tf. Finally, application to urine samples further demonstrated the potential of probe **21** for the diagnosis of IgA nephropathy and HSPN.

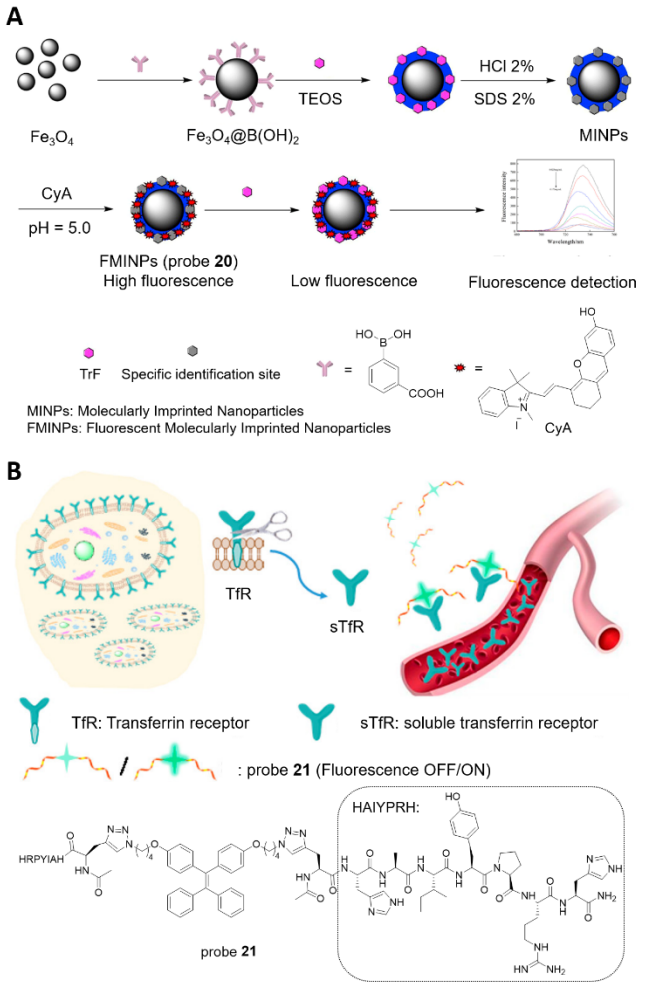

Scheme 6. A) Synthetic route to probe **20**. Adapted with permission from ref. 102. Copyright 2018 Elsevier B.V. B) Schematics of the sensing mechanism and chemical structure of probe **21**. Adapted with permission from ref. 104. Copyright 2018 American Chemical Society.

Both MIT and specific recognition peptide make the sensing process highly specific. Moreover, the fluorescent 'turn-on' probe **21** is more favourable for its merits of low background noise, good linear correlation, and broad detection range. Thus, the AIE probe **21** has great potential to be used for the diagnosis of IgA nephropathy and HSPN.

3. Application of Fluorescence Technologies in the Detection of Novel KDBs

Currently, sCr is the most used biomarker of renal function. However, it is far from an ideal biomarker for the early and accurate diagnosis of kidney diseases. Given the limitations of traditional KDBs, different urinary and serum proteins, molecules, or even microRNAs have been investigated in the past decade as potential novel biomarkers for kidney diseases. Since space is limited, we will only briefly introduce several selected novel biomarkers in this section.

3.1 *N*-acetyl-β-D-glucosaminidase

N-acetyl-β-D-glucosaminidase (NAG) is a type of hydrolytic lysosomal enzyme present in many tissues of our bodies. It presents a high concentration in the lysosomes of proximal tubular cells. Due to its high molecular weight (130 kDa), NAG cannot be filtered through the glomerulus. Therefore, it is usually excreted in very low amount in urine as the consequence of normal exocytosis. However, during proximal tubule injury, the secretion of NAG in urine will increase significantly. Thus, NAG can serve as a biomarker of renal tubule related disease such as nephritic syndrome, drug-induced acute kidney injury (DIAKI), diabetes, etc.[105]

In recent years, NAG has drawn more and more attention due to its early and accurate diagnosis of kidney injury. Up to now, a colorimetric assay kit has been developed for measuring NAG activity in clinical.[106] However, this method requires a laborious procedure, and exhibits low sensitivity and high background noise in many cases. In 2019, Yan, Tian et al. reported an enzyme-activated fluorescent probe (**22**) for the selective detection of NAG activity in a DIAKI mice model and NAG level in human urine.[107] As can be seen in **Scheme 7**, resorufin (7-hydroxy-3H-phenoxazin-3-one) was selected as the fluorescence reporter due to its long wavelength emission and high quantum yield, and *N*-acetyl-β-D-glucosaminide acts as the NAG reactive group. After the alkylation of the 7-hydroxy group, the fluorescence intensity of resorufin was effectively quenched due to the weaken ICT effect. However, once the reactive substituent cleaved by NAG, the fluorescence of resorufin was restored. Therefore, probe **22** displays extremely low background, high sensitivity, and good specificity towards NAG. Most recently, Pu's group successfully developed a series of fluorescent probes for real-time imaging of early-stage biomarkers of DIAKI in murine models.[108] The superoxide anion ($O_2^{\bullet-}$), NAG and caspase-3 were selected as the target biomarkers because they can represent oxidative stress, lysosomal damage and cellular apoptosis, respectively. As shown in **Scheme 7**, the NAG probe **23** mainly contains three parts: (2-hydroxypropyl)-β-cyclodextrin as the renal clearance moiety, hemi-cyanine as the NIR fluorescence reporter, and *N*-acetyl-β-D-glucosaminide as the NAG reactive moiety. Due to

the substitution of a NAG reactive group, the electron donating ability of the aromatic hydroxyl group was weakened, which greatly reduced the fluorescent of probe **23** in its intrinsic state. After reacting with NAG, the fluorescence of probe **23** was obviously enhanced with an emission peak at 720 nm. Moreover, only negligible fluorescence change of probe **23** can be found towards other enzyme interferents, manifesting its high specificity. Thanks to the prominent performance in NAG sensing, the authors further studied the probe's applications in real-time NIR fluorescence imaging and in vitro diagnosis. The real-time imaging of living mice receiving cisplatin treatment at a nephrotoxic dosage showed that probe **23** could be lit up at 16 h post-treatment. For the in vitro detection, two different methods were applied. In the online urinalysis, probe **23** was injected to mice at different timepoints, and the excreted urine with probe molecules inside was measured to check the existence of NAG. In the offline method, probe **23** was incubated in the urine from drug-treated mice to inspect the corresponding biomarker. The results indicated that probe **23** can identified DIAKI approximately 24~72 h earlier than the clinical NGAL, Cystatin C and β2-microglobulin assays in a cisplatin-induced AKI mouse mode. Following this work, the authors reported one duplex reporter **24** based on the same design strategy.[109] As shown in **Scheme 7**, this probe has a similar structure as probe **23** except for an additional $O_2^{\bullet-}$ activatable chemiluminescent moiety. After injecting probe **24** into living mice, it specifically travels to the kidneys and sends chemiluminescent and photoluminescent signals to report real-time $O_2^{\bullet-}$ and NAG levels, respectively. Such a design can be used to study the fundamental correlation between $O_2^{\bullet-}$ and NAG during the progression of DIAKI.

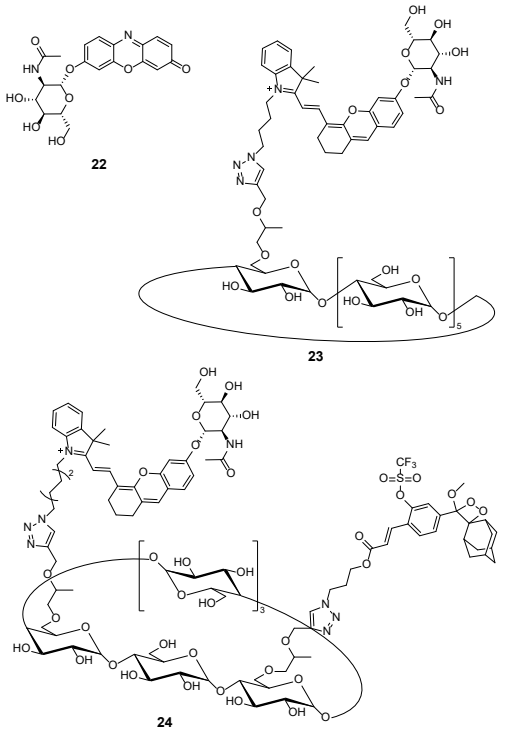

Scheme 7. Chemical structures of NAG probes **22**-**24**.

In summary, these three NAG probes all apply *N*-acetyl-β-D-glucosaminide as the specific recognition group which can be selectively cleaved by NAG. Besides, the fluorescence of the fluorophores can be easily modulated by the removing of substituents from the hydroxyl group. As a result, all of them exhibits satisfying sensing results towards NAG. The development of novel easily accessible fluorescent probes with high sensitivity for NAG is still highly desired due the significant role of NAG.

3.2 Cystatin C

Cystatin C is a non-glycosylated protein with a low molecular weight of around 13.3 kDa. It can be produced by all nucleated cells in humans and exists in virtually all tissues and body fluids. As a potent inhibitor of cysteine protease, the major function of cystatin C is to prevent the breakdown of proteins and reduce the risk of diseases.[110] Besides, since the production rate of cystatin C is relatively constant and it can only be removed through renal glomerular filtration, cystatin C can also be used as a marker for estimating the GFR. Compared with sCr, the serum level of cystatin C is less dependent on age, gender, race, muscle mass, and inflammation.[111] Therefore, the serum cystatin C has been regarded as an ideal marker to evaluate renal glomerular injury. Unlike in serum, the concentration of cystatin C in urine is extremely low. This can be ascribed to the reabsorption and degradation of cystatin C in proximal tubules. Once the proximal tubules are injured due to certain diseases, the level of cystatin C in urine will increase accordingly. Thus, urine cystatin C can be applied to reflect the function of renal tubulars as well.[112]

In the past decades, there have been many immunoassays reported for the measurement of cystatin C, such as particle enhanced turbidimetric immunoassay (PETIA), enzyme and fluorophore labelled heterogeneous immunoassays, etc.[113] Despite these methods are sensitive and selective, the immunoassays are usually very expensive and require sophisticated antibody preparation, which greatly limits their application. In 2013, Lin et al. reported an immune-independent assay based on fluorescent AuNCs for the detection of cystatin C.[114] The working mechanism of this assay is elucidated in **Scheme 8A**. Initially, the BSA templated AuNCs (**25**) emit strong fluorescence at 680 nm when excited at 340 nm. After adding papain, a cysteine protease, the fluorescence was quenched due to the digestion of BSA. Moreover, as aforementioned, cystatin C is an efficient cysteine protease inhibitor, with which the fluorescence of **25**-papain mixture would be restored. Thus, the concentration of cystatin C can be quantified by measuring the fluorescence intensity of **25**-papain mixture. After performing this assay in buffer environment, an LDR of 0.025-2.0 μg/mL and a LOD of 4.0 ng/mL were obtained with good specificity. The LOD is more than 40-fold lower than that of commercial immune-based methods such as PETIA (0.17 mg/mL). Encouraged by these results, the authors further studied its performance in urinalysis. The results turned out that both the BSA-AuNCs assay and PETIA gave satisfactory recovery and precision. Moreover, due to the lower LOD and simpler synthesis, the BSA-AuNCs assay has the potential to be applied

in clinical detection of cystatin C. In 2016, a similar work was reported by Zhao and co-workers.[115] Instead of using AuNC, the researchers synthesized PbS semiconductor QDs employing BSA as the bio-template (**Scheme 8B**). The as prepared PbS@BSA QDs (probe **26**) showed NIR emission at around 813 nm under the excitation at 450 nm. Since the Pb^{2+} was mainly bounded with the carboxyl groups and amino groups of BSA, BSA plays a critical role in maintaining the fluorescence of probe **26**. Furthermore, by the introduction of papain, the concentration of cystatin C can be quantified through the same strategy of probe **25**. Finally, probe **26** was shown to have excellent performance in practical detection of cystatin C in serum samples.

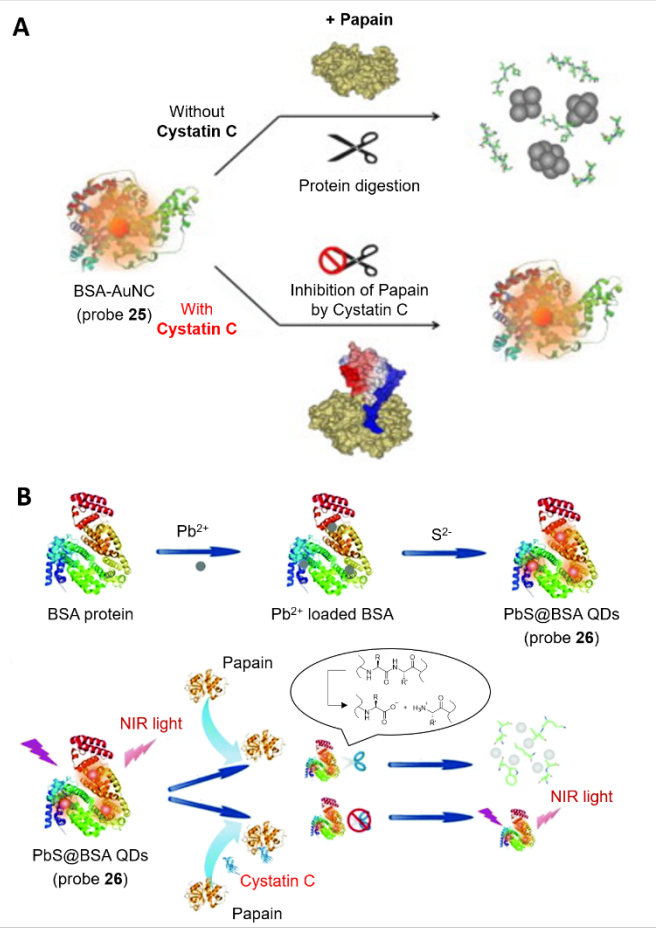

Scheme 8. Schematics of the sensing mechanisms of A) probe **25** and B) probe **26**. A) Adapted with permission from ref. 114. Copyright 2012 Elsevier B.V. B) Adapted with permission from ref. 115. Copyright 2016 The Royal Society of Chemistry.

3.3 Neutrophil gelatinase-associated lipocalin, NGAL

Neutrophil gelatinase-associated lipocalin (NGAL), also known as lipocalin-2, or siderocalin, is a secretory glycoprotein belonging to the lipocalin superfamily comprising of 178 amino acids with a total molecular weight of ~25 kDa. The physiological function of NGAL mainly includes transporting hydrophobic ligands across cell membranes, modulating immune responses, and promoting epithelial cell differentiation.[116] Normally, NGAL from renal tissues is expressed in a low rate to stimulate the differentiation of kidney progenitor cells into renal tubular epithelial cells ensuring the normal growth of the kidney. However, in early AKI cases, both serum and urinary NGAL levels increase rapidly.[117] According to previous research, NGAL elevation can be detected in 3 h after renal injury and reaches the maximum in 6-12 h.[118] Therefore, NGAL can be used as a novel biomarker for early diagnosis of AKI.

As one of the most promising KDBs under investigation, many detection methods for NGAL have been developed, for example Western Blot, polymerase chain reaction (PCR), enzyme linked immune sorbent assay (ELISA) and so on. However, due to their disadvantages of tedious operation and high cost, the clinical application of NGAL as a biomarker is limited. Therefore, it is necessary to establish a reliable detection method for NGAL. In 2016, Sugawara and co-workers reported a giant unilamellar vesicles (GUVs) containing Rhodamine 6G (R6G-GUVs, probe **27**, **Scheme 9A**) as a fluorescent marker for immunoassay of NGAL.[119] Firstly, probe **27** was synthesized from a lipid mixture of 1,2-diphytanoyl-sn-glycero-3-phosphocholine, cholesterol, and 1,2-dioleoyl-sn-glycero-3-phosphoethanolamine through the electro-formation method.[120] Secondly, the GUV based probe was functionalized with NGAL antibody (anti-NGAL) through the bioconjugation reaction between amino groups from probe **27** and carboxyl acid groups from anti-NGAL. Afterwards, the substrate used for immobilizing antibody was prepared based on surface modification of cover slips followed by anti-NGAL conjugation. Finally, the fluorescence-based sandwich-type immunoassay was successfully established. In a regular test procedure, the anti-NGAL functionalized probe was linked to the anti-NGAL slip in the presence of NGAL. After adding Triton X-100, the liposome structure of probe **27** decomposed immediately releasing Rhodamine 6G into the outer solution. Due to the ACQ effect, the fluorescence of Rhodamine 6G was quenched when encapsulated with a high concentration in the GUVs, while was lit up when comes to dilute solutions. Therefore, the variation of fluorescence signal can be used for the detection of NGAL. From the data provided in this work, the detected fluorescence intensity increased linearly with NGAL concentration in the range from 0.1 to 10 pg/mL. Moreover, the LOD of this method was 0.08 pg/mL which is far superior to those of the conventional ELISA methods, graphene-based immunoassay, and particle-enhanced turbidimetric assay. After confirming the negligible interference effect from HSA, γ-globulin, Tf, and haptoglobin, probe **27** was further applied in detecting NGAL from human serum. Although the recovery value was acceptable, the detection result was larger than that obtained from the ELISA method. This may be explained by the various forms of NGAL and different configurations of the antibody. In summary, this assay with extremely low LOD may find some applications in detecting other biomarkers with low levels at the early stage of disease.

Recently, Yu, Tian and co-workers developed a polydopamine nanosphere (PDANSs)/fluorescent aptamer nanocomplex for rapid and sensitive detection of NGAL.[121] The aptamers used in this work are single-stranded DNA/RNA oligonucleotides which

have a high affinity to NGAL. A commercialized fluorescent dye 5-carboxyfluorescein (5-FAM) was labelled to the aptamer generating the NGAL probe **28** (**Scheme 9B**). Due to the π–π interaction between aptamer and PDANSs, probe **28** was adsorbed onto the surface of PDANSs forming a nanocomplex and enabling the fluorescence quenching through the FRET principle. However, the weak π–π interaction can be easily broken down through adding NGAL which has a higher affinity towards the aptamer. As a result, the fluorescence of probe **28** will be recovered accordingly. Furthermore, a higher recovery of probe **28** can be obtained via the introduction of DNase I which can digest the dissociated aptamers and release NGAL to bind to another probe on PDANSs. Hence, the sensitivity of probe **28** can be effectively increased. As proved by the authors, in the presence of 10 U DNase I, the fluorescence intensity of PDANSs/**28** nanocomplex at 520 nm increased linearly with the concentration of NGAL, giving a LDR of 12.5 to 400 pg/mL and a LOD of 6.25 pg/mL which was 5 times lower than that obtained in the absence of DNase I. Finally, this simple and rapid assay was proved to detect urinary NGAL for the early prediction of AKI.

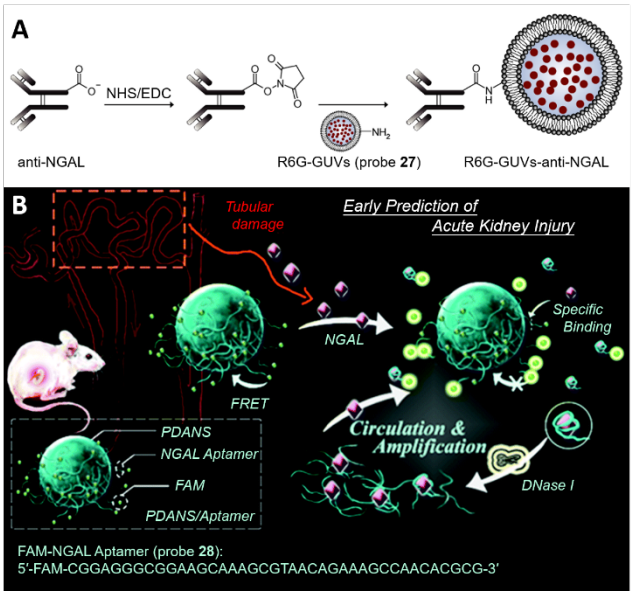

Scheme 9. A) Schematic illustration for functionalizing R6G-GUVs (probe **27**) with anti-NGAL. Adapted with permission from ref. 119. Copyright 2016 Elsevier Inc. B) Schematic illustration of the PDANSs/probe **28** nanocomplex coupled with a DNase I assisted recycling amplification strategy for the detection of NGAL during the process of AKI. Adapted with permission from ref. 121. Copyright 2020 The Royal Society of Chemistry.

3.4 Kidney injury molecule-1, KIM-1

Kidney injury molecule-1 (KIM-1), also termed as Hepatitis A virus cellular receptor-1 (HAVCR-1) and T-cell immunoglobulin and mucin domain 1 (TIM-1), is a type 1 transmembrane protein comprised of an extracellular segment containing a mucin domain and immunoglobulin-like domains and a cytosolic segment containing a tyrosine kinase phosphorylation moiety. It has basal expression in a normal kidney but is significantly upregulated in renal tubular epithelial cells damaged during toxic or ischemic induced AKI. Meanwhile, the extracellular domain of KIM-1 will be released into urine shortly after the renal injury. Compared with other KDBs, KIM-1 has shown great superiority in the early prediction of AKI. Thus, KIM-1 is promising to become a useful tool for detection and treatment of AKI at early stage.

Currently, the most commonly used method for KIM-1 detection is ELISA. In 2016, a fluorescence-linked immunosorbent assay (FLISA) for KIM-1 expression detection was developed by Gaurer et al.[122] Instead of using the biotin-streptavidin-peroxidase complex method in ELISA, the FLISA applies fluorescent dye labelled antibodies to bind with KIM-1 attached to the immobilized antibodies. After incubation and wash, the fluorescence signal can indicate the expression of KIM-1. Due to the use of KIM-1 antibody, both ELISA and FLISA methods are high-cost. Most recently, Lee and co-workers reported a related work which applied a fluorescent dye labelled peptide for the detection of KIM-1.[123] The specific peptide CNWMINKEC was firstly determined by the phage display technique. After this peptide was synthesized, it was further conjugated at the amino terminus with fluorescein isothiocyanate (FITC) or FPR675 NIR fluorescence dye, producing the KIM-1 fluorescent probe **29** and **30**, respectively. In order to check the binding of peptide CNWMINKEC to KIM-1, probe **29** was incubated in a plate coated with KIM-1. After washing the plate, fluorescence intensity was measured using a fluorometer. The results indicated that peptide CNWMINKEC has a higher affinity towards KIM-1 than other control peptides. Therefore, probe **29** was further applied in the detection of KIM-1 high expressing tumor cells such as 769-P, A498, and ACHN renal tumor cells, and A549 lung tumor cells. Flow cytometry analysis demonstrated that the CNWMINKEC peptide has an excellent binding ability to KIM-1 high expressing tumor cells. In terms of cytotoxicity, CNWMINKEC peptide did not affect the viability of 769-P and HEK-293 cells significantly, suggesting its good biocompatibility. Besides, this peptide was stable in the serum for up to 24 h. Thus, probe **30** was further applied in the in vivo imaging and detection of KIM-1 overexpressing tumors of a mouse model. These findings suggest that the peptide CNWMINKEC is a promising aptamer for designing KIM-1 probe for detection and imaging KIM-1 protein or KIM-1 overexpressing tumors.

3.5 Other novel biomarkers

Except for the KDBs mentioned above, there are many other novel biomarkers emerged in the past decades. These biomarkers include liver fatty acid-binding protein (L-FABP), interleukin-18 (IL-18), retinol binding protein 4 (RBP4), Tamm-Horsfall glycoprotein (THP), γ-glutamyl transpeptidase (GGT), glutathione S-transferase (GST), asymmetric dimethylarginine (ADMA), microRNA, etc.[124-128] Since very few fluorescent probes for the detection of these biomarkers were reported, a simple introduction of several selected biomarkers will be given in this section.

IL-18 is a proinflammatory cytokine that was first characterized in the middle of 1990s.[126] The level of IL-18 in the urine from

patients with ischemic acute tubular necrosis was demonstrated to be higher than that from patients with other renal diseases.[129] Besides, elevated levels of urinary IL-18 can be detected 48 h before the diagnosis of ischemic AKI using serum creatinine as the biomarker.[14] Therefore, IL-18 is a promising biomarker for early diagnosis of ischemic AKI. As previously demonstrated, immunoassays can provide good sensitivity and specificity for the detection of many proteins. However, due to its low abundance in plasma or urine, the levels of cytokine may be below the LOD of traditional immunoassay. Therefore, Hahm and co-workers proposed a novel zinc oxide nanorods (ZnONRs) platform for the ultrasensitive detection of cytokines in urine.[130] In this work, IL-18 and tumor necrosis factor-α (TNFα) were used as cytokine models. A sandwich immunoassay was adopted using ZnONRs modified Si plate as the substrate and fluorescent dye labelled antibodies (probe **31**) as the reporter. The overall procedures for IL-18 and TNFα detection were illustrated in **Scheme 10A**. Identical assays were also performed on substrates made from PS, PMMA and PS-*b*-PVP. Subsequently, fluorescence signals were measured, showing that the detection sensitivity of ZnONRs modified substrates was higher than those of the polymeric substrates. The authors explained that this result can be ascribed to the fluorescence enhancing effect of ZnONRs on vicinal fluorophores. Furthermore, this ZnONRs platform was applied in the detection of IL-18 in both PBS buffer and urine. Finally, the LOD was found to be in the 1-10 fg/mL range, which exceeded that of conventional assays by 3-4 orders of magnitude. This ultralow LOD makes the ZnONRs assay beneficial for the sensitive detection of protein biomarkers at extremely low concentrations.

Retinol binding protein 4 (RBP4), is a small molecular (21 kDa) transporter protein for retinol (vitamin A alcohol). After delivering the retinol to target tissues, RBP4 will be filtered by the renal glomerulus, and reabsorbed and decomposed by proximal renal tubules, excreting very small amount into the urine. However, in the disease of proximal tubule, a large amount of RBP4 together with other small molecular proteins will exist in urine resulting in the 'tubular proteinuria'. Especially in the renal Fanconi Syndrome (FS), a high level of RBP4 can be found in the tubular proteinuria.[131] Therefore, urinary RBP4 (uRBP4) appears to be a robust biomarker for proximal renal tubular diseases. Currently, measurement of urinary RBP4 is very difficult due to the various forms of RBP4 and non-linearity between patient samples and assay standards. In order to solve this problem, Norden and coworkers firstly applied a 'top-down' MS approach which determined that uRBP4 in FS contains intact plasma RBP4 and C-terminal truncated RBP4, desL-RBP4 and desLL-RBP4 in molar ratio of 2:2:1.[132] Afterwards, a Dissociation-Enhanced Lanthanide Fluorescent Immunoassay (DELFIA®) was developed using a capture monoclonal antibody (mAb), a biotinylated detection mAb, a streptavidin conjugated europium, and a free plasma RBP4 standard. Due to the replacement of polyclone antibody (pAb) with mAb, the new DELFIA® technique fully overcame the problem of non-linearity, providing good sensitivity (LOD = 1 μg/L) and LDR of 1 to 500 μg/L. Finally, clinical application of the mAb-based DELFIA® assay was validated in 3 groups of patients and improved discrimination was obtained than the original pAb assay.

Glutathione S-transferase (GST) is an important phase II metabolic enzyme which plays a critical role in toxicity reduction. It is broadly distributed in all organs of human's body, especially in the cytosol. In kidney, GST has a specific distribution with α form presented only in the proximal tubules, and π from presented in the distal tubules and collecting ducts. In 1995, Sundberg et al. reported that GST may serve as a diagnostic marker for renal disease.[133] Under normal health conditions, the urinary level of GST is extremely low, while in renal tubular diseases, the amount of GST in urine will increase remarkedly. Consequently, it is highly desired to develop an effective GST detection assay for the early diagnosis of related diseases. In 2019, Xiao and co-workers reported fluorescent conjugated polymer nanoparticles (FCPNPs) for the detection of GST.[134] The principle of their design is illustrated in **Scheme 10B**. Firstly, water-soluble FCPNPs were synthesized from fluorescent conjugated polymer poly[(9,9-dioctylfluorenyl-2,7-diyl)-*alt*-co-1,4-benzo-2,1'-3-thiadiazole] (PFBT) and amphiphilic copolymer poly(styrene-co-maleic anhydride) (PSMA), according to a reported nanoprecipitation method. After modified with GSH through hydrogen bonding, the produced FCPNPs-GSH (probe **32**) behaved as an energy donor. Meanwhile, polyethylenimine (PEI) capped gold nanoparticles (GNPs) were synthesized via a one-pot reaction, producing positively charged GNPs@PEI which served as an energy receptor. Due to electrostatic interaction, GNPs@PEI can bind to FCPNPs-GSH and cause fluorescence quenching through the FRET effect. Afterwards, the particles of FCPNPs-GSH + GNPs@PEI complex were applied for sensing GST. When GST was introduced, due to its high binding affinity towards GSH, the GNPs@PEI on the surface of FCPNPs-GSH would be replaced by GST. Consequently, the fluorescence of FCPNPs-GSH will be recovered, indicating the presence of GST. It is noteworthy that the concentration of GST was quantified using the Single-Particle Enumeration (SPE) assay which monitored the number of fluorescent particles by the total internal reflection fluorescence (TIRF) microscopy imaging technique. With this assay, a good LDR of 0.01 to 6 μg/mL and a low LOD of 1.03 ng/mL were obtained for GST detection. Finally, application of this approach in real urine samples was performed and satisfying recoveries (97.5 to 106.5%) was obtained demonstrating its potential in clinical application.

The last novel KDB discussed here is γ-glutamyl transpeptidase (GGT), also known as γ-glutamyl transferase, a transferase that transfers the γ-glutamyl groups from molecules such as GSH to an acceptor which can be an amino acid, a peptide or water.[135] GGT is involved in several important physiological processes such as GSH metabolism and xenobiotic detoxification. GGT levels can also be applied to indicate many diseases including diabetes, asthma, and cancer.[136] As a brush border enzyme present in the proximal renal tubules, GGT can also be used as a KDB. The increased levels of GGT in urine reflect the loss of brush border integrity which is caused by kidney injury. In 2016, Hou et al. reported a turn-on fluorescent probe for GGT detection based on the AIE effect.[137] As shown in **Scheme 10C**,

the AIE probe **33** comprises a TPE core and two γ-glutamyl amide groups. The γ-glutamyl amide groups not only provided probe **33** with good water solubility, but also functioned as recognition units for GGT. As a result, probe **33** displayed good solubility in aqueous media with no aggregates formed and no fluorescence emitted. However, when GGT was added, the γ-glutamyl amides were cleaved through enzymatic reaction, and hydrophobic TPE derivatives were generated, forming aggregates with strong blue fluorescence. Thus, probe **33** was applied in the detection of GGT in both buffer media and human serum samples. The results showed that probe **33** has good photostability, selectivity, and sensitivity (LOD 0.59 U/L in PBS buffer) in GGT test. Finally, due to its low cytotoxicity, probe **33** was further used for fluorescence imaging of GGT in living A2780 cells.

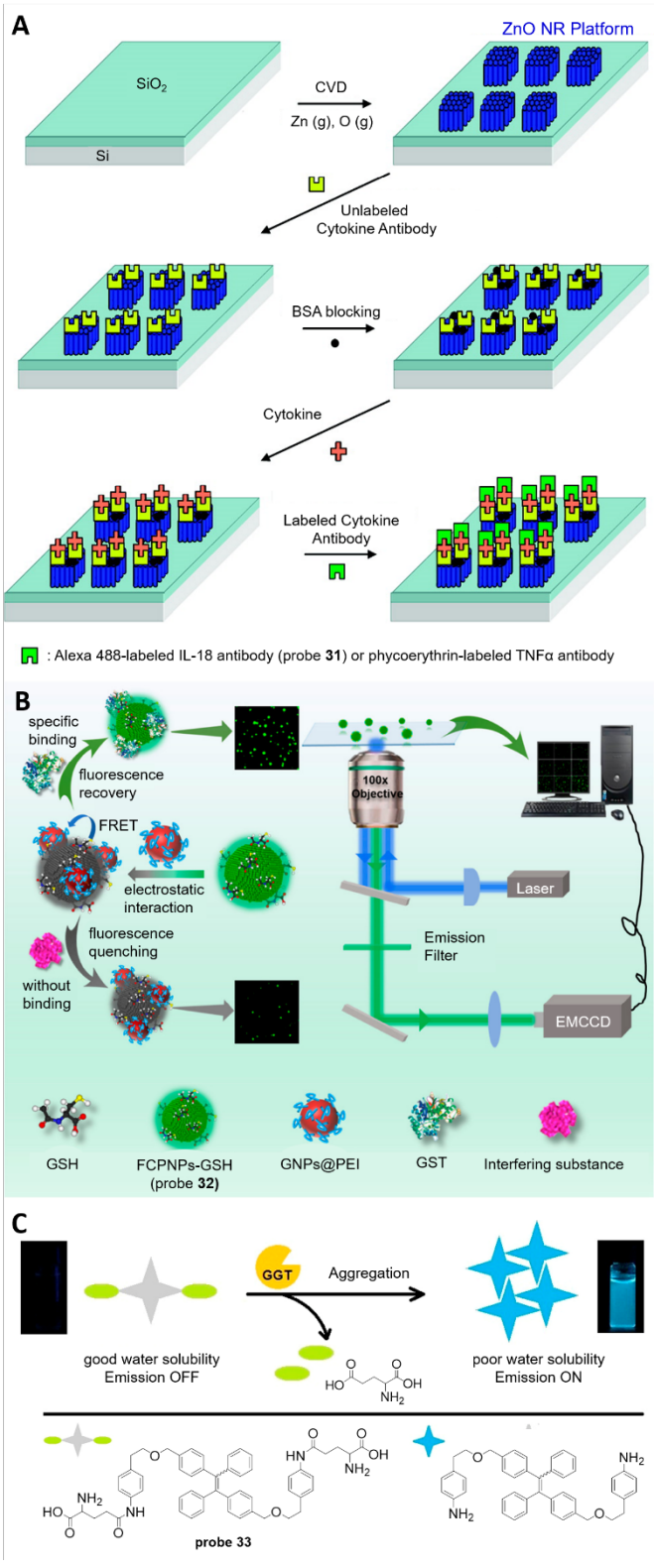

Scheme 10. A) Schematic illustration showing the overall assay scheme for the detection of cytokines. Adapted with permission from ref. 130. Copyright 2008 American Chemical Society. B) Schematic diagram of the light path for single-particle imaging and the principle of SPE assay for GST detection. Adapted with permission from ref. 134. Copyright 2019 American Chemical Society. C) Chemical structure of probe **33** and schematic illustration of its fluorescent detection for GGT. Adapted with permission from ref. 137. Copyright 2016 Elsevier B.V.

4. Conclusion and outlook

In this review, recent advances of fluorescence technologies in the detection of KDBs were summarized. Through selecting representative biomarkers, the chemical structure designs of probe molecules and ingenious detection process have been thoroughly introduced. It can be observed from the examples that fluorescent materials including novel AIEgens and metal nanoclusters, and classical organic fluorophores have been extensively applied in the detection of traditional KDBs such as albumin, creatinine, Tf, and sTfR. However, for novel KDBs, only a few examples of fluorescence technique have been reported. The novel biomarkers discussed in this paper include NAG, Cystatin C, NGAL, KIM-1, IL-18, RBP4, GST, and GGT. Among them, antibodies are indispensable for the detection of IL-18 and RBP4, which makes the corresponding assays tedious and costly. For the other novel KDBs, satisfying detection performance can be realized through analytes' specific binding to or cleavage of recognition groups from probe molecules, which can turn on fluorescent signal as a response. These results display a promising potential of fluorescence technology in the detection of novel KDBs.

To date, many different fluorescence techniques have been applied to the detection of KDBs. However, there are still many crucial aspects to be considered for further development of fluorescence technology in KDB sensing. These challenges include but not limited to the followings: 1) Since some of the fluorescent probes appear to be promising in clinical application, further studies are needed to validate their competence in clinical tests; 2) Recognition units for KIM-1, IL-18 and RBP4 are in high demand for the design of relevant fluorescent probes; 3) Due to outstanding advances over conventional ACQ dye, AIEgens merit more attention in developing new fluorescent probes for novel KDBs; 4) Current test methods are either conducted in solution or need complex procedures. An easy to operate test mode, such as paper strips, needs to be established for personal use. In conclusion, advanced fluorescence detection technologies combined with

novel KDBs will bring us great benefit in the early diagnosis of kidney diseases and contribute to human health.

Conflicts of interest

There are no conflicts to declare.

Acknowledgements

We acknowledge the Australia-China Science and Research Fund, Joint Research Centre on Personal Health Technologies for support.

Notes and references

1. E. A. Hartung, Biomarkers and surrogate endpoints in kidney disease, *Pediatr. Nephrol.*, 2016, **31**, 381-391.
2. J. V. Donadio and J. P. Grande, IgA nephropathy, *N. Engl. J. Med.*, 2002, **347**, 738-748.
3. J. S. Cameron, Lupus Nephritis, *J. Am. Soc. Nephrol.*, 1999, **10**, 413-424.
4. L. D. Byham-Gray, J. D. Burrowes and G. M. Chertow, *Nutrition in kidney disease*, Springer, New York, 2014.
5. K. Kalantar-Zadeh and P. K.-T. Li, Strategies to prevent kidney disease and its progression, *Nat. Rev. Nephrol.*, 2020, **16**, 129-130.
6. O. J. Wouters, D. J. O'Donoghue, J. Ritchie, P. G. Kanavos and A. S. Narva, Early chronic kidney disease: Diagnosis, management and models of care, *Nat. Rev. Nephrol.*, 2015, **11**, 491-502.
7. L. A. Stevens and A. S. Levey, Current status and future perspectives for CKD testing, *Am. J. Kidney Dis.*, 2009, **53**, 17-26.
8. S. P. Clavant, T. M. Osicka and W. D. Comper, Albuminuria: Its importance in disease detection, *Lab. Medicine*, 2007, **38**, 35-38.
9. C. Thomas and L. Thomas, Renal failure--measuring the glomerular filtration rate, *Dtsch. Arztebl. Int.*, 2009, **106**, 849-854.
10. J. G. Fried and M. A. Morgan, Renal imaging: Core curriculum 2019, *Am. J. Kidney Dis.*, 2019, **73**, 552-565.
11. J. V. Bonventre, Current biomarkers in kidney disease: Dawning of a new era, *ASN Kidney News*, 2014, 7-8.
12. A. Sakhuja and E. V. Lerma, Novel biomarkers of renal function introduction and overview, *Medscape*, 2019, 1-13.
13. J. Rysz, A. Gluba-Brzozka, B. Franczyk, Z. Jablonowski and A. Cialkowska-Rysz, Novel biomarkers in the diagnosis of chronic kidney disease and the prediction of its outcome, *Int. J. Mol. Sci.*, 2017, **18**, 1702.
14. I. Wu and C. R. Parikh, Screening for kidney diseases: Older measures versus novel biomarkers, *Clin. J. Am. Soc. Nephrol.*, 2008, **3**, 1895-1901.
15. W. Fu and J. Huang, Overview of researches on biomarkers of kidney disease, *Sect. Clin. Biochem. & Lab Med. Foreign Med. Sci.*, 2004, **25**, 97-98.
16. L. Sun, H. Ma, L. Dong and M. Zhu, Biomarkers of kidney disease and injury, *Med. J. Air Force*, 2015, **31**, 321-324.
17. N. Wang, Y. Feng and X. Zhang, Advances in the study of biomarkers of kidney diseases, *Int. J. Lab Med.*, 2015, **36**, 1128-1131.
18. Y. Tong, X. Huang, M. Lu, B.-Y. Yu and J. Tian, Prediction of drug-induced nephrotoxicity with a hydroxyl radical and caspase light-up dual-signal nanoprobe, *Anal. Chem.*, 2018, **90**, 3556-3562.
19. D. Sasaki, A. Yamada, H. Umeno, H. Kurihara, S. Nakatsuji, S. Fujihira, K. Tsubota, M. Ono, A. Moriguchi, K. Watanabe and J. Seki, Comparison of the course of biomarker changes and kidney injury in a rat model of drug-induced acute kidney injury, *Biomarkers*, 2011, **16**, 553-566.
20. R. A. Star, Treatment of acute renal failure, *Kidney Int.*, 1998, **54**, 1817-1831.
21. M. Yu, J. Zhou, B. Du, X. Ning, C. Authement, L. Gandee, P. Kapur, J.-T. Hsieh and J. Zheng, Noninvasive staging of kidney dysfunction enabled by renal-clearable luminescent gold nanoparticles, *Angew. Chem. Int. Ed.*, 2016, **55**, 2787-2791.
22. A. Prasanna de Silva, H. Q. N. Gunaratne, T. Gunnlaugsson, A. J. M. Huxley, C. P. McCoy, J. T. Rademacher and T. E. Rice, Signaling recognition events with fluorescent sensors and switches, *Chem. Rev.*, 1997, **97**, 1515-1566.
23. X. Lim, The nanoscale rainbow, *Nature*, 2016, **531**, 26-28.
24. U. Resch-Genger, M. Grabolle, S. Cavaliere-Jaricot, R. Nitschke and T. Nann, Quantum dots versus organic dyes as fluorescent labels, *Nat. Methods*, 2008, **5**, 763-775.
25. B. N. G. Giepmans, S. R. Adams, M. H. Ellisman and R. Y. Tsien, The fluorescent toolbox for assessing protein location and function, *Science*, 2006, **312**, 217-224.
26. I. L. Medintz, H. T. Uyeda, E. R. Goldman and H. Mattoussi, Quantum dot bioconjugates for imaging, labelling and sensing, *Nat. Mater.*, 2005, **4**, 435-446.
27. B. J. B., *Photophysics of Aromatic Molecules*, Wiley-Interscience London, 1970.
28. J. Luo, Z. Xie, J. W. Y. Lam, L. Cheng, H. Chen, C. Qiu, H. S. Kwok, X. Zhan, Y. Liu, D. Zhu and B. Z. Tang, Aggregation-induced emission of 1-methyl-1,2,3,4,5-pentaphenylsilole, *Chem. Commun.*, 2001, 1740-1741.
29. Y. Hong, J. W. Y. Lam and B. Z. Tang, Aggregation-induced emission, *Chem. Soc. Rev.*, 2011, **40**, 5361-5388.
30. J. Mei, N. L. C. Leung, R. T. K. Kwok, J. W. Y. Lam and B. Z. Tang, Aggregation-induced emission: Together we shine, united we soar!, *Chem. Rev.*, 2015, **115**, 11718-11940.
31. R. Hu, A. Qin and B. Z. Tang, AIE polymers: Synthesis and applications, *Prog. Polym. Sci.*, 2020, **100**, 101176.
32. M. Gao and B. Z. Tang, Fluorescent sensors based on aggregation-induced emission: Recent advances and perspectives, *ACS Sens.*, 2017, **2**, 1382-1399.
33. Z. Zhao, H. Zhang, J. W. Y. Lam and B. Z. Tang, Aggregation-induced emission: New vistas at the aggregate level, *Angew. Chem. Int. Ed.*, 2020, **59**, 9888-9907.
34. X. Ni, X. Zhang, X. Duan, H.-L. Zheng, X.-S. Xue and D. Ding, Near-infrared afterglow luminescent aggregation-induced emission dots with ultrahigh tumor-to-liver signal ratio for promoted image-guided cancer surgery, *Nano Lett.*, 2019, **19**, 318-330.
35. C. Chen, X. Ni, S. Jia, Y. Liang, X. Wu, D. Kong and D. Ding, Massively evoking immunogenic cell death by focused mitochondrial oxidative stress using an AIE luminogen with a twisted molecular structure, *Adv. Mater.*, 2019, **31**, 1904914.

36. C. Chen, X. Ni, H.-W. Tian, Q. Liu, D.-S. Guo and D. Ding, Calixarene-based supramolecular AIE dots with highly inhibited nonradiative decay and intersystem crossing for ultrasensitive fluorescence image-guided cancer surgery, *Angew. Chem. Int. Ed.*, 2020, **59**, 10008-10012.
37. G. Feng, G.-Q. Zhang and D. Ding, Design of superior phototheranostic agents guided by Jablonski diagrams, *Chem. Soc. Rev.*, 2020, **49**, 8179-8234.
38. C. Chen, H. Ou, R. Liu and D. Ding, Regulating the photophysical property of organic/polymer optical agents for promoted cancer phototheranostics, *Adv. Mater.*, 2020, **32**, 1806331.
39. S. Bolisetty and A. Agarwal, Urine albumin as a biomarker in acute kidney injury, *Am. J. Physiol. Renal Physiol.*, 2011, **300**, F626-F627.
40. S. H. Ba Aqeel, A. Sanchez and D. Batlle, Angiotensinogen as a biomarker of acute kidney injury, *Clin. Kidney J.*, 2017, **10**, 759-768.
41. S. Lopez-Giacoman and M. Madero, Biomarkers in chronic kidney disease, from kidney function to kidney damage, *World J. Nephrol.*, 2015, **4**, 57-73.
42. E. V. Schrezenmeier, J. Barasch, K. Budde, T. Westhoff and K. M. Schmidt-Ott, Biomarkers in acute kidney injury - pathophysiological basis and clinical performance, *Acta Physiol.*, 2017, **219**, 556-574.
43. J. Zhou, X. Ouyang, X. Cui, T. R. Schoeb, L. E. Smythies, M. R. Johnson, L. M. Guay-Woodford, A. B. Chapman and M. Mrug, Renal CD14 expression correlates with the progression of cystic kidney disease, *Kidney Int.*, 2010, **78**, 550-560.
44. V. S. Vaidya, M. A. Ferguson and J. V. Bonventre, Biomarkers of acute kidney injury, *Annu. Rev. Pharmacol. Toxicol.*, 2008, **48**, 463-493.
45. W. R. Zhang and C. R. Parikh, Biomarkers of acute and chronic kidney disease, *Annu. Rev. Physiol.*, 2019, **81**, 309-333.
46. N. Piazzon, F. Bernet, L. Guihard, W. N. Leonhard, S. Urfer, D. Firsov, H. Chehade, B. Vogt, S. Piergiovanni, D. J. Peters, O. Bonny and D. B. Constam, Urine Fetuin-A is a biomarker of autosomal dominant polycystic kidney disease progression, *J. Transl. Med.*, 2015, **13**, 103.
47. M. E. Wasung, L. S. Chawla and M. Madero, Biomarkers of renal function, which and when?, *Clin. Chim. Acta*, 2015, **438**, 350-357.
48. T. Isakova, H. Xie, W. Yang, D. Xie, A. H. Anderson, J. Scialla, P. Wahl, O. M. Gutiérrez, S. Steigerwalt, J. He, S. Schwartz, J. Lo, A. Ojo, J. Sondheimer, C.-Y. Hsu, J. Lash, M. Leonard, J. W. Kusek, H. I. Feldman and M. Wolf, Fibroblast growth factor 23 and risks of mortality and end-stage renal disease in patients with chronic kidney disease, *JAMA*, 2011, **305**, 2432-2439.
49. M. Meersch, C. Schmidt, H. Van Aken, S. Martens, J. Rossaint, K. Singbartl, D. Görlich, J. A. Kellum and A. Zarbock, Urinary TIMP-2 and IGFBP7 as early biomarkers of acute kidney injury and renal recovery following cardiac surgery, *PLoS One*, 2014, **9**, e93460.
50. K. L. Connor and L. Denby, MicroRNAs as non-invasive biomarkers of renal disease, *Nephrol. Dial. Transplant. Plus*, 2019, 1-2.
51. C.-L. Lin, P.-H. Lee, Y.-C. Hsu, C.-C. Lei, J.-Y. Ko, P.-C. Chuang, Y.-T. Huang, S.-Y. Wang, S.-L. Wu, Y.-S. Chen, W.-C. Chiang, J. Reiser and F.-S. Wang, MicroRNA-29a promotion of nephrin acetylation ameliorates hyperglycemia-induced podocyte dysfunction, *J. Am. Soc. Nephrol.*, 2014, **25**, 1698-1709.
52. T. Wada, K. Furuichi, N. Sakai, Y. Iwata, K. Yoshimoto, M. Shimizu, S. I. Takeda, K. Takasawa, M. Yoshimura, H. Kida, K.-I. Kobayashi, N. Mukaida, T. Naito, K. Matsushima and H. Yokoyama, Up-regulation of monocyte chemoattractant protein-1 in tubulointerstitial lesions of human diabetic nephropathy, *Kidney Int.*, 2000, **58**, 1492-1499.
53. G. Ramesh, O. Kwon and K. Ahn, Netrin-1: A novel universal biomarker of human kidney injury, *Transplant. Proc.*, 2010, **42**, 1519-1522.
54. C. Suwanpen, P. Nouanthong, V. Jaruvongvanich, K. Pongpirul, W. A. Pongpirul, A. Leelahavanichkul and T. Kanjanabuch, Urinary podocalyxin, the novel biomarker for detecting early renal change in obesity, *J. Nephrol.*, 2016, **29**, 37-44.
55. B. E. Ghoul, T. Squalli, A. Servais, C. Elie, V. Meas-Yedid, C. Trivint, J. Vanmassenhove, J.-P. Grünfeld, J.-C. Olivo-Marin, E. Thervet, L.-H. Noël, D. Prié and F. Fakhouri, Urinary procollagen III aminoterminal propeptide (PIIINP): A fibrotest for the nephrologist, *Clin. J. Am. Soc. Nephrol.*, 2010, **5**, 205-210.
56. R. Relford, J. Robertson and C. Clements, Symmetric dimethylarginine: Improving the diagnosis and staging of chronic kidney disease in small animals, *Vet. Clin. Small Anim.*, 2016, **46**, 941-960.
57. C. R. Parikh and S. G. Mansour, Perspective on clinical application of biomarkers in AKI, *J. Am. Soc. Nephrol.*, 2017, **28**, 1677-1685.
58. A. Kalani, A. Mohan, M. M. Godbole, E. Bhatia, A. Gupta, R. K. Sharma and S. Tiwari, Wilm's tumor-1 protein levels in urinary exosomes from diabetic patients with or without proteinuria, *PLoS One*, 2013, **8**, e60177.
59. C. Donadio and L. Bozzoli, Urinary β-trace protein: A unique biomarker to screen early glomerular filtration rate impairment, *Medicine*, 2016, **95**, e5553.
60. G. Fanali, A. Masi, V. Trezza, M. Marino, M. Fasano and P. Ascenzi, Human serum albumin: From bench to bedside, *Mol. Aspects Med.*, 2012, **33**, 209-290.
61. X. M. He and D. C. Carter, Atomic structure and chemistry of human serum albumin, *Nature*, 1992, **358**, 209-215.
62. G. Sudlow, D. J. Birkett and D. N. Wade, The characterization of two specific drug binding sites on human serum albumin, *Mol. Pharmacol.*, 1975, **11**, 824-832.
63. O. K. Abou-Zied and O. I. K. Al-Shihi, Characterization of subdomain IIA binding site of human serum albumin in its native, unfolded, and refolded states using small molecular probes, *J. Am. Chem. Soc.*, 2008, **130**, 10793-10801.
64. T. Lü, K. Zhu and B. Liu, Recent advances of organic fluorescent probes for detection of human serum albumin, *Chinese J. Org. Chem.*, 2019, **39**, 2786-2795.
65. J.-F. Xu, Y.-S. Yang, A.-Q. Jiang and H.-L. Zhu, Detection Methods and Research Progress of Human Serum Albumin, *Crit. Rev. Anal. Chem.*, 2020, DOI: 10.1080/10408347.2020.1789835.
66. Y. Tu, Y. Yu, Z. Zhou, S. Xie, B. Yao, S. Guan, B. Situ, Y. Liu, R. T. K. Kwok, J. W. Y. Lam, S. Chen, X. Huang, Z. Zeng and B. Z. Tang, Specific and quantitative detection of albumin in biological fluids by tetrazolate-functionalized water-

soluble AIEgens, *ACS Appl. Mater. Interfaces*, 2019, **11**, 29619-29629.

67. H. Li, Q. Yao, J. Fan, J. Du, J. Wang and X. Peng, An NIR fluorescent probe of uric HSA for renal diseases warning, *Dyes and Pigments*, 2016, **133**, 79-85.
68. S. Xie, A. Y. H. Wong, S. Chen and B. Z. Tang, Fluorogenic detection and characterization of proteins by aggregation-induced emission methods, *Chem. Eur. J.* , 2019, **25**, 5824-5847.
69. H. Lu, K. Wang, B. Liu, M. Wang, M. Huang, Y. Zhang and J. Yang, Systematic oligoaniline-based derivatives: ACQ–AIE conversion with a tunable insertion effect and quantitative fluorescence “turn-on” detection of BSA, *Mater. Chem. Front.*, 2019, **3**, 331-338.
70. N. Dey, B. Maji and S. Bhattacharya, Motion-induced changes in emission as an effective strategy for the ratiometric probing of human serum albumin and trypsin in biological fluids, *Chem. Asian J.*, 2018, **13**, 664-671.
71. Z. Zhu, B. Song, J. Yuan and C. Yang, Enabling the triplet of tetraphenylethene to sensitize the excited state of Europium(III) for protein detection and time-resolved luminescence imaging, *Adv. Sci.*, 2016, **3**, 1600146.
72. L. Wang, L. Yang, L. Zhu, D. Cao and L. Li, Synthesis, characterization and fluorescence “turn-on” detection of BSA based on the cationic poly(diketopyrrolopyrrole-co-ethynylfluorene) through deaggregating process, *Sens. Actuators B Chem.*, 2016, **231**, 733-743.
73. K. Suenaga, R. Yoshii, K. Tanaka and Y. Chujo, Sponge-type emissive chemosensors for the protein detection based on boron ketoiminate-modifying hydrogels with aggregation-induced blueshift emission property, *Macromol. Chem. Phys.*, 2016, **217**, 414-421.
74. Y. Hong, C. Feng, Y. Yu, J. Liu, J. W. Y. Lam, K. Q. Luo and B. Z. Tang, Quantitation, visualization, and monitoring of conformational transitions of human serum albumin by a tetraphenylethene derivative with aggregation-induced emission characteristics, *Anal. Chem.*, 2010, **82**, 7035-7043.
75. H. Tong, Y. Hong, Y. Dong, M. Haussler, J. W. Y. Lam, Z. Li, Z. Guo, Z. Guo and B. Z. Tang, Fluorescent "light-up" bioprobes based on tetraphenylethylene derivatives with aggregation-induced emission characteristics, *Chem. Commun.*, 2006, 3705-3707.
76. J. Tong, T. Hu, A. Qin, J. Z. Sun and B. Z. Tang, Deciphering the binding behaviours of BSA using ionic AIE-active fluorescent probes, *Faraday Discuss.*, 2017, **196**, 285-303.
77. J. Li, J. Wu, F. Cui, X. Zhao, Y. Li, Y. Lin, Y. Li, J. Hu and Y. Ju, A dual functional fluorescent sensor for human serum albumin and chitosan, *Sens. Actuators B Chem.*, 2017, **243**, 831-837.
78. Z. L. Wang, K. Ma, B. Xu, X. Li and W. J. Tian, A highly sensitive “turn-on” fluorescent probe for bovine serum albumin protein detection and quantification based on AIE-active distyrylanthracene derivative, *Sci. China Chem.*, 2013, **56**, 1234-1238.
79. W. Li, D. Chen, H. Wang, S. Luo, L. Dong, Y. Zhang, J. Shi, B. Tong and Y. Dong, Quantitation of albumin in serum using "turn-on" fluorescent probe with aggregation-enhanced emission characteristics, *ACS Appl. Mater. Interfaces*, 2015, **7**, 26094-26100.
80. Y. Yu, Y. Huang, F. Hu, Y. Jin, G. Zhang, D. Zhang and R. Zhao, Self-assembled nanostructures based on activatable red fluorescent dye for site-specific protein probing and conformational transition detection, *Anal. Chem.*, 2016, **88**, 6374-6381.
81. Z. Luo, T. Lv, K. Zhu, Y. Li, L. Wang, J. J. Gooding, G. Liu and B. Liu, Paper-based ratiometric fluorescence analytical devices towards point-of-care testing of human serum albumin, *Angew. Chem. Int. Ed.*, 2020, **59**, 3131-3136.
82. Q. Sun, W. Wang, Z. Chen, Y. Yao, W. Zhang, L. Duan and J. Qian, A fluorescence turn-on probe for human (bovine) serum albumin based on the hydrolysis of a dioxaborine group promoted by proteins, *Chem. Commun.*, 2017, **53**, 6432-6435.
83. M. Wyss and R. Kaddurah-Daouk, Creatine and creatinine metabolism, *Physiol. Rev.*, 2000, **80**, 1107-1213.
84. E. Lamb, *Clinical Biochemistry*, Oxford University Press, New York, 2 edn., 2011.
85. M. Jaffe, Ueber den Niederschlag, welchen Pikrinsäure in normalem harn erzeugt und über eine neue reaction des kreatinins, *Z. Phys. Chem. (N F)*, 1886, **10**, 391-400.
86. O. Folin and J. L. Morris, On the determination of creatinine and creatine in urine, *J. Biol. Chem.*, 1914, **17**, 469-473.
87. J. R. Delanghe and M. M. Speeckaert, Creatinine determination according to Jaffe—what does it stand for?, *Nephrol. Dial. Transplant. Plus*, 2011, **4**, 83-86.
88. T. Küme, B. Sağlam, C. Ergon and A. R. Sisman, Evaluation and comparison of Abbott Jaffe and enzymatic creatinine methods: Could the old method meet the new requirements?, *J. Clin. Lab. Anal.*, 2018, **32**, e22168.
89. G. L. Myers, W. G. Miller, J. Coresh, J. Fleming, N. Greenberg, T. Greene, T. Hostetter, A. S. Levey, M. Panteghini, M. Welch and J. H. Eckfeldt, Recommendations for Improving Serum Creatinine Measurement: A Report from the Laboratory Working Group of the National Kidney Disease Education Program, *Clin. Chem.*, 2006, **52**, 5-18.
90. T. Chen, N. Xie, L. Viglianti, Y. Zhou, H. Tan, B. Z. Tang and Y. Tang, Quantitative urinalysis using aggregation-induced emission bioprobes for monitoring chronic kidney disease, *Faraday Discuss.*, 2017, **196**, 351-362.
91. Z. Luo, X. Yuan, Y. Yu, Q. Zhang, D. T. Leong, J. Y. Lee and J. Xie, From aggregation-induced emission of Au(I)-thiolate complexes to ultrabright Au(0)@Au(I)-thiolate core-shell nanoclusters, *J. Am. Chem. Soc.*, 2012, **134**, 16662-16670.
92. M. S. Mathew and K. Joseph, Green synthesis of gluten-stabilized fluorescent gold quantum clusters: Application as turn-on sensing of human blood creatinine, *ACS Sustainable Chem. Eng.*, 2017, **5**, 4837-4845.
93. H. Zhang, Z. Zhao, P. R. McGonigal, R. Ye, S. Liu, J. W. Y. Lam, R. T. K. Kwok, W. Z. Yuan, J. Xie, A. L. Rogach and B. Z. Tang, Clusterization-triggered emission: Uncommon luminescence from common materials, *Mater. Today*, 2020, **32**, 275-292.
94. R. Rajamanikandan and M. Ilanchelian, Protein-protected red emittive copper nanoclusters as a fluorometric probe for highly sensitive biosensing of creatinine, *Anal. Methods*, 2018, **10**, 3666-3674.
95. R. Jalili and A. Khataee, Aluminum(III) triggered aggregation-induced emission of glutathione-capped copper nanoclusters as a fluorescent probe for creatinine, *Mikrochim. Acta*, 2018, **186**, 29.
96. A. F. Sierra, D. Hernandez-Alonso, M. A. Romero, J. A. Gonzalez-Delgado, U. Pischel and P. Ballester, Optical

supramolecular sensing of creatinine, *J. Am. Chem. Soc.*, 2020, **142**, 4276-4284.

97. S. S. Nanda, S. S. An and D. K. Yi, Measurement of creatinine in human plasma using a functional porous polymer structure sensing motif, *Int. J. Nanomedicine*, 2015, **10**, 93-99.

98. S. Pal, S. Lohar, M. Mukherjee, P. Chattopadhyay and K. Dhara, A fluorescent probe for the selective detection of creatinine in aqueous buffer applicable to human blood serum, *Chem. Commun.*, 2016, **52**, 13706-13709.

99. Y. Fu, L. Shi, Z. Zhao, D. Yang, Q. Li, Y. Tang and X. Zhang, Ethyl ‐ substituted thioflavin T as a fluorescent probe for detecting the conformation of transferrin, *Chemistry Select*, 2019, **4**, 10270-10275.

100. W. R. Alley, Jr., B. F. Mann and M. V. Novotny, High-sensitivity analytical approaches for the structural characterization of glycoproteins, *Chem. Rev.*, 2013, **113**, 2668-2732.

101. L. Chen, X. Wang, W. Lu, X. Wu and J. Li, Molecular imprinting: Perspectives and applications, *Chem. Soc. Rev.*, 2016, **45**, 2137-2211.

102. Y.-D. Zhang, Q.-W. Huang, C. Ma, X.-Y. Liu and H.-X. Zhang, Magnetic fluorescent molecularly imprinted nanoparticles for detection and separation of transferrin in human serum, *Talanta*, 2018, **188**, 540-545.

103. S. E. Delanghe, M. M. Speeckaert, H. Segers, K. Desmet, J. Vande Walle, S. V. Laecke, R. Vanholder and J. R. Delanghe, Soluble transferrin receptor in urine, a new biomarker for IgA nephropathy and Henoch-Schonlein Purpura Nephritis, *Clin. Biochem.*, 2013, **46**, 591-597.

104. R. Zhang, S. H. P. Sung, G. Feng, C. J. Zhang, Kenry, B. Z. Tang and B. Liu, Aggregation-induced emission probe for specific turn-on quantification of soluble transferrin receptor: An important disease marker for iron deficiency anemia and kidney diseases, *Anal. Chem.*, 2018, **90**, 1154-1160.

105. A. Mohammadi-Karakani, S. Asgharzadeh-Haghighi, M. Ghazi-Khansari and R. Hosseini, Determination of urinary enzymes as a marker of early renal damage in diabetic patients, *J. Clin. Lab. Anal.*, 2007, **21**, 413-417.

106. A. Noto, Y. Ogawa, S. Mori, M. Yoshioka, T. Kitakaze, T. Hori, M. Nakamura and T. Miyake, Simple, rapid spectrophotometry of urinary N-acetyl-beta-D-glucosaminidase, with use of a new chromogenic substrate, *Clin. Chem.*, 1983, **29**, 1713-1716.

107. F. Yan, X. Tian, Z. Luan, L. Feng, X. Ma and T. D. James, NAG-targeting fluorescence based probe for precision diagnosis of kidney injury, *Chem. Commun.*, 2019, **55**, 1955-1958.

108. J. Huang, J. Li, Y. Lyu, Q. Miao and K. Pu, Molecular optical imaging probes for early diagnosis of drug-induced acute kidney injury, *Nat. Mater.*, 2019, **18**, 1133-1143.

109. J. Huang, Y. Lyu, J. Li, P. Cheng, Y. Jiang and K. Pu, A renal-clearable duplex optical reporter for real-time imaging of Contrast-Induced Acute Kidney Injury, *Angew. Chem. Int. Ed.*, 2019, **58**, 17796-17804.

110. M. Abrahamson, M. Alvarez-Fernandez and C.-M. Nathanson, Cystatins *Biochem. Soc. Symp.*, 2003, **70**, 179-199.

111. A. Bökenkamp, M. Domanetzki, R. Zinck, G. Schumann, D. Byrd and J. Brodehl, Cystatin C—A new marker of glomerular filtration rate in children independent of age and height, *Pediatrics*, 1998, **101**, 875-881.

112. J. L. Koyner, M. R. Bennett, E. M. Worcester, Q. Ma, J. Raman, V. Jeevanandam, K. E. Kasza, M. F. O'Connor, D. J. Konczal, S. Trevino, P. Devarajan and P. T. Murray, Urinary cystatin C as an early biomarker of Acute Kidney Injury following adult cardiothoracic surgery, *Kidney Int.*, 2008, **74**, 1059-1069.

113. J. Kyhse-Andersen, C. Schmidt, G. Nordin, B. Andersson, P. Nilsson-Ehle, V. Lindström and A. Grubb, Serum cystatin C, determined by a rapid, automated particle-enhanced turbidimetric method, is a better marker than serum creatinine for glomerular filtration rate, *Clin. Chem.*, 1994, **40**, 1921-1926.

114. H. Lin, L. Li, C. Lei, X. Xu, Z. Nie, M. Guo, Y. Huang and S. Yao, Immune-independent and label-free fluorescent assay for Cystatin C detection based on protein-stabilized Au nanoclusters, *Biosens. Bioelectron.*, 2013, **41**, 256-261.

115. J. Tao, P. Zhao and Q. Zeng, The determination of cystatin C in serum based on label-free and near-infrared light emitted PbS@BSA QDs, *J. Mater. Chem. B*, 2016, **4**, 4258-4262.

116. G. S. Santiago-Sanchez, V. Pita-Grisanti, B. Quinones-Diaz, K. Gumpper, Z. Cruz-Monserrate and P. E. Vivas-Mejia, Biological functions and therapeutic potential of lipocalin 2 in cancer, *Int. J. Mol. Sci.*, 2020, **21**, 4365.

117. K. M. Schmidt-Ott, K. Mori, A. Kalandadze, J.-Y. Li, N. Paragas, T. Nicholas, P. Devarajan and J. Barasch, Neutrophil gelatinase-associated lipocalin-mediated iron traffic in kidney epithelia, *Curr. Opin. Nephrol. Hypertens.*, 2006, **15**, 442-449.

118. T. L. Nickolas, M. J. O'Rourke, J. Yang, M. E. Sise, P. A. Canetta, N. Barasch, C. Buchen, F. Khan, K. Mori, J. Giglio, P. Devarajan and J. Barasch, Sensitivity and specificity of a single emergency department measurement of urinary neutrophil gelatinase–associated lipocalin for diagnosing Acute Kidney Injury, *Ann. Intern. Med.*, 2008, **148**, 810-819.

119. M. Sakamoto, A. Shoji and M. Sugawara, Giant unilamellar vesicles containing Rhodamine 6G as a marker for immunoassay of bovine serum albumin and lipocalin-2, *Anal. Biochem.*, 2016, **505**, 66-72.

120. D. J. Estes and M. Mayer, Giant liposomes in physiological buffer using electroformation in a flow chamber, *Biochim. Biophys. Acta.*, 2005, **1712**, 152-160.

121. Y. Hu, X.-a. Yu, Y. Zhang, R. Zhang, X. Bai, M. Lu, J. Li, L. Gu, J.-H. Liu, B.-Y. Yu and J. Tian, Rapid and sensitive detection of NGAL for the prediction of acute kidney injury via a polydopamine nanosphere/aptamer nanocomplex coupled with DNase I-assisted recycling amplification, *Analyst*, 2020, **145**, 3620-3625.

122. S. Gauer, A. Urbschat, N. Gretz, S. C. Hoffmann, B. Kränzlin, H. Geiger and N. Obermüller, Kidney Injury Molecule-1 is specifically expressed in cystically-transformed proximal tubules of the PKD/Mhm (cy/+) rat model of polycystic kidney disease, *Int. J. Mol. Sci.*, 2016, **17**, 802.

123. M. E. Haque, F. Khan, L. Chi, S. Gurung, S. M. P. Vadevoo, R.-W. Park, D.-K. Kim, S. K. Kim and B. Lee, A phage display-identified peptide selectively binds to Kidney Injury Molecule-1 (KIM-1) and detects KIM-1-overexpressing tumors in vivo, *Cancer Res. Treat.*, 2019, **51**, 861-875.

124. Y. Xu, Y. Xie, X. Shao, Z. Ni and S. Mou, L-FABP: A novel biomarker of kidney disease, *Clin. Chim. Acta.*, 2015, **445**, 85-90.

125. P. Trionfini, A. Benigni and G. Remuzzi, MicroRNAs in kidney physiology and disease, *Nat. Rev. Nephrol.*, 2015, **11**, 23-33.
126. P. Cen, C. Walther, K. W. Finkel and R. J. Amato, in *Renal Disease in Cancer Patients*, Elsevier, 2014, pp. 21-38.
127. M. Y. Alsagaff, M. Thaha, M. Aminuddin, R. Yogiarto, M. Yogiantoro and Y. Tomino, Asymmetric dimethylarginine: A novel cardiovascular risk factor in end-stage renal disease, *J. Int. Med. Res.*, 2012, **40**, 340-349.
128. F. Serafini-Cessi, N. Malagolini and D. Cavallone, Tamm-Horsfall Glycoprotein: Biology and clinical relevance, *Am. J. Kidney Dis.*, 2003, **42**, 658-676.
129. C. R. Parikh, A. Jani, V. Y. Melnikov, S. Faubel and C. L. Edelstein, Urinary interleukin-18 is a marker of human acute tubular necrosis, *Am. J. Kidney Dis.*, 2004, **43**, 405-414.
130. V. Adalsteinsson, O. Parajuli, S. Kepics, A. Gupta, W. B. Reeves and J.-i. Hahm, Ultrasensitive detection of cytokines enabled by nanoscale ZnO arrays, *Anal. Chem.*, 2008, **80**, 6594-6601.
131. A. G. Norden, S. J. Scheinman, M. M. Deschodt-Lanckman, M. Lapsley, J. L. Nortier, R. V. Thakker, R. J. Unwin and O. Wrong, Tubular proteinuria defined by a study of Dent's (CLCN5 mutation) and other tubular diseases, *Kidney Int.*, 2000, **57**, 240-249.
132. K. A. Burling, P. R. Cutillas, D. Church, M. Lapsley and A. G. W. Norden, Analysis of molecular forms of urine retinol-binding protein in fanconi syndrome and design of an accurate immunoassay, *Clin. Chim. Acta.*, 2012, **413**, 483-489.
133. A. G. Sundberg, R. Nilsson, E.-L. Appelkvist and G. Dallner, ELISA procedures for the quantitation of glutathione transferases in the urine, *Kidney Int.*, 1995, **48**, 570-575.
134. Y. Han, T. Chen, Y. Li, L. Chen, L. Wei and L. Xiao, Single-particle enumeration-based sensitive glutathione s-transferase assay with fluorescent conjugated polymer nanoparticle, *Anal. Chem.*, 2019, **91**, 11146-11153.
135. S. S. Tate and A. Meister, γ-Glutamyl transpeptidase from kidney, *Meth. Enzymol.*, 1985, **113**, 400-419.
136. Z. Luo, L. Feng, R. An, G. Duan, R. Yan, H. Shi, J. He, Z. Zhou, C. Ji, H. Y. Chen and D. Ye, Activatable near-infrared probe for fluorescence imaging of γ-glutamyl transpeptidase in tumor cells and in vivo, *Chem. Eur. J.* , 2017, **23**, 14778-14785.
137. X. Hou, F. Zeng and S. Wu, A fluorescent assay for γ-glutamyltranspeptidase via aggregation induced emission and its applications in real samples, *Biosens. Bioelectron.*, 2016, **85**, 317-323.